

BEACH EROSION BOARD
OFFICE OF THE CHIEF OF ENGINEERS

APPROXIMATE RESPONSE OF
WATER LEVEL ON A SLOPING SHELF
TO A WIND FETCH WHICH MOVES
TOWARDS SHORE

TECHNICAL MEMORANDUM NO. 83



APPROXIMATE RESPONSE OF WATER LEVEL ON A SLOPING SHELF TO A WIND FETCH WHICH MOVES TOWARDS SHORE



DEPARTMENT OF THE ARMY
CORPS OF ENGINEERS
TECHNICAL MEMORANDUM NO. 83

JUNE 1956

FOREWORD

High water and waves accompanying storms of hurricane intensity have periodically caused great damage along the Atlantic and Gulf coasts of the United States. Damage figures have risen with each succeeding great storm as more and more development of the shore areas has been made, reaching, for example, an estimated 200 million dollars in the Narragansett Bay area, including Providence, Rhode Island, for the 1954 hurricane Carol. Adequate, and economic, design of shore structures to prevent or mitigate this damage requires accurate prediction of water levels for any possible future storm. Complete understanding of the development of storm surges along an open coast has not yet been realized. Certain simplifications and assumptions may be made, however, and these lead to various possible solutions. One such solution for determining the dynamic storm tide potential is given here, based on a simplified hydrography (vertical slopes at shore and deep ocean and a gradual straight-line slope between), one dimensional linear hydrodynamic equations, constant storm speed, approach perpendicular to the coast, boundary conditions of zero flow at the shore and zero flow and elevation initially at the ocean edge, and consideration of wind stress only. The equations are solved by the method of characteristics and are applied to the Narragansett Bay area. Similar application to other areas may be made, however, if the same offshore depth ratio (0.1) applies.

The report was prepared at the Agricultural and Mechanical College of Texas by Robert O. Reid, an Associate Professor at that institution, in pursuance of contract DA-49-055-Civ-eng-56-4 between the Beach Erosion Board and the Texas A & M Research Foundation. The report is a result of work sponsored by the Corps of Engineers as a part of its responsibilities in hurricane damage prevention, as outlined in Public Law 71, 84th Congress. Funds were supplied through the New England Division of the Corps as a part of a comprehensive study of hurricane prevention for the southern New England shore.

Views and conclusions stated in this report are not necessarily those of the Beach Erosion Board.

This report is published under authority of Public Law 166, 79th Congress, approved July 31, 1945.

<u>CONTENTS</u>	<u>Page</u>
List of Figures	ii
List of Tables	iii
List of Symbols	iv
Abstract	1
I. INTRODUCTION	1
II. METHOD OF CHARACTERISTICS	3
1. The Presumed Equations of Motion	3
2. Bottom Topography	3
3. Transformation of the Differential Equations	5
4. The Method of Characteristics Applied to the First Approximation Equations	7
Free Waves	8
Forced Waves	10
5. Boundary Conditions	11
6. Determination of the Forced Water Level at Shore	11
7. The Model Fetch	13
8. Graphical Integration Technique	15
III. LIMITING CASES	18
1. Steady State	18
2. Uniform Wind Field	20
IV. HIGHER ORDER APPROXIMATIONS	23
1. Equations for the Higher Order Approximations	23
2. Steady State	24
3. Second Approximation for the Case of $F = L$, $V/C = 0.5$	25
4. Modified Condition at the Edge of the Shelf	27
V. THE RESPONSE DIAGRAM	31
1. First Approximation Response Diagram	31
2. Modified Response Diagram	31
3. Use of the Response Diagram	35
VI. EVALUATION OF STORM TIDE POTENTIAL FOR PAST STORMS	40
1. Evaluation of F and W	40
2. The Storm Tide Potentials ^{III}	41
3. Comparison of R and F	46
4. Suggested Method for Selection of the Most Severe Storm	46
References	47

LIST OF FIGURES

<u>Figure</u>		<u>Page</u>
1	Mean Bottom Profile off Narragansett Bay -----	4
2-A	Schematic Characteristic Diagram for a Free Wave ----	9
2-B	Schematic Characteristic Diagram for a Forced Wave ($V < \bar{C}$) -----	9
2-C	Schematic Characteristic Diagram for a Forced Wave ($V > \bar{C}$) -----	9
3-A	Selected Force Field on x^* , t^* diagram -----	14
3-B	Schematic of Graphical Integration -----	14
3-C	Isolines of G for a Uniform Wind Field -----	14
4	Z_0 Versus t^* for $V = \bar{C}$ and Various F/L -----	17
5	Z_0 Versus t^* for $F = L/2$ and Various V/\bar{C} -----	17
6	Steady State Z_m Versus F/L , First Approximation and Exact Solution -----	19
7	Z_m (First Approximation) Versus VT/F for a Uniform Wind Field -----	19
8	Field of First Approximation Values of Z for $V/\bar{C} = 0.5$, $F = L$ -----	26
9	Field of First Approximation Values of Y for $V/\bar{C} = 0.5$, $F = L$ -----	26
10	Plot of First and Second Approximation of Z_0 for $V/\bar{C} = 0.5$, $F = L$ -----	28
11	Comparison of Water Levels and Volume Trans- ports for Modified Edge Condition with those of First Approximation. -----	30
12	Composite Plot of First Approximation Values of Z_m Versus VT/F for Different F/L -----	34
13	Response Diagram: Isolines of S Versus F/L and V/\bar{C} -	36
14	Relative Time of Maximum Water Level at Shore -----	38
15	Generation Stage of Surge for the Case $V/\bar{C} = 0.5$, $F = L$	39
16	Schematic of Storm Showing Angles θ , ϕ and ψ -----	40

LIST OF FIGURES (Cont'd)

<u>Figure</u>		<u>Page</u>
17	Plot of WW Along Line Parallel to Path through Region of Peak Wind Speed for Hurricane of September 21, 1938 -----	42
18	Plot of WW Along Line Parallel to Path through Region of Peak Wind Speed for Hurricane of September 14, 1944 -----	42
19	Plot of WW Along Line Parallel to Path through Region of Peak Wind Speed for Hurricane of August 30, 1954 -	42
20	Surface Wind Isolines for Hurricane of September 21, 1938 - 1500 E.S.T. -----	43
21	Example of Computation of Z for $F = 2L$, $V = \bar{C}$ -----	44
22	Half Life Versus VT/F for Different Fetches -----	45

LIST OF TABLES

<u>Table</u>		<u>Page</u>
1-A	Summary of Calculations for First Approximation Values of Z_m , $t_m^* - t_w^*$, and Δt^* for finite F -----	32
1-B	Summary of Calculations for First Approximation Values of Z_m , $t_m^* - t_w^*$, and Δt^* for uniform wind ($F = \infty$) -	33
2	Correction Factor to be Multiplied by Z_m Values -----	35
3	Computed Storm Tide Potentials for the New England Hurricanes of 1938, 1944 and 1954 (Carol) -----	41

LIST OF SYMBOLS

A	Area under curve of $G(t')$ see Figure 3-B.
A_n	Coefficients in the series for Z, case of uniform wind, eqs. (51).
B_n	Coefficients in the series for Z, case of uniform wind, eqs. (51).
C	\sqrt{gh} , velocity of progress of a free, long wave for the depth h.
\bar{C}	Mean free wave speed, eq.(5 iv).
C_0	$\sqrt{gh_0}$
C_1	$\sqrt{gh_1}$
f	Dimensionless driving force (positive towards shore), eq.(4 v).
F	Fetch length.
g	Acceleration of gravity.
G	$y^{-1/2}f$.
h	Depth of water at position x, in the absence of the storm surge.
h_0	Effective depth at shore.
h_1	Effective depth at the edge of the shelf.
k	Resistance coefficient.
k_n	Coefficient defined by eq.(50).
K	Dimensionless coefficient, eq.(75).
ln	Natural logarithm notation.
L	Width of the continental shelf.
m	Slope of the continental shelf.
M_1	Scale modulus for the t' scale.
M_2	Scale modulus for the G scale.
M_3	Scale modulus for the basic grid. eq.(38).
n	A positive integer.
p_a	Sea level atmospheric pressure at position x and time t.
p_n	Coefficient defined by eq.(52 i).
Q	Volume transport in the x direction through a vertical section of depth h and unit width transverse to the x-axis.
r	Correction factor (ratio of the exact steady state solution to the first approximation steady solution).
R	Distance from storm center to region of maximum wind.
S	Response factor for η , see eq.(73), (76) or (77); depends upon V/\bar{C} and F/L (Fig. 13). ^m
t'	t/T , dimensionless time variable.
t	Time.
t_1'	A selected starting time for the characteristics, eqs.(24) etc.

t_e'	Relative time of passage of end of fetch at shore.
t_m'	Relative time of occurrence of maximum water level (initial surge) at shore.
t_w'	Relative time of maximum shoreward wind speed at shore.
T	Travel time for a free, long wave to cross the shelf, eq.(5i).
U	A characteristic parameter of the fetch where ρU^2 represents the maximum value of shoreward wind stress in the fetch.
v	Dimensionless storm speed, eq.(35).
V	Shoreward velocity of the storm.
W	Surface wind speed (at about 30 to 40 feet above sea level).
W_m	$\sqrt{(WW)_{x \text{ max}}}$
W_x	Component of wind velocity towards shore.
x	Horizontal coordinate taken normal to shore, positive seaward.
x'	x/x_1 , dimensionless distance variable.
x_0	Position of the shore line.
x_1	Position of edge of the shelf.
x_0'	x_0/x_1 (taken as 0.1 in the numerical work).
y	$\sqrt{x/x_1}$ (dimensionless).
y_0	$\sqrt{x_0/x_1}$
Y	Dimensionless volume transport variable eq.(4 iv).
Y'	First approximation of Y .
Y''	Correction which when added to Y' gives the second approximation for Y .
Y'''	Correction which when added to $Y' + Y''$ gives the third approximation for Y .
Y_0	Value of Y at shore at time t (taken as zero).
Y_1	Value of Y at edge of shelf at time t' .
Z	Dimensionless water level variable eq.(4 iii).
Z_m	Maximum value of Z at shore.
Z_0	Value of Z at shore at time t' .
Z_1	Value of Z at edge of shelf at time t' .
Z'	First approximation of Z .
Z''	Correction which when added to Z' gives the second approximation for Z .

Z'''	Correction which when added to $Z'' + Z'$ gives the third approximation for Z .
α_0	Half fetch length in dimensionless form ($F/2x_1$).
β_n	Angle in radians defined by eq.(52ii).
γ	Dimensionless parameter associated with the characteristics, eq. (4 vi).
δ	An angle in radians defined by eq. (55 ii).
$\Delta t'$	Half life of initial surge in dimensionless form (see Fig. 22).
η	Anomaly of water level above predicted astronomical tide at position x and time t .
η_m	Maximum value of η at shore.
θ	Angle between wind vector and x axis, see Fig. 16.
π	3.14159...
ρ	Density of sea water.
ρ'	Density of air at sea level.
τ	Wind stress (tangential force per unit area) at position x and time t .
ϕ	Orientation angle, see Fig. 16.
ψ	Angle of inward inclination of wind vector, see Fig. 16.

APPROXIMATE RESPONSE OF WATER LEVEL ON A SLOPING SHELF
TO A WIND FETCH WHICH MOVES DIRECTLY TOWARDS SHORE

by
R. O. Reid
Associate Professor of Oceanography
A. & M. College of Texas
College Station, Texas

ABSTRACT

The following report describes a procedure for evaluating the approximate response characteristics of water level at the shore of a sloping shelf due to a wind fetch moving directly onshore. The theory is based upon the linear one-dimensional wave equation and employs the method of characteristics as a means of solution by graphical technique. A total of about 55 separate cases for different values of fetch length and storm speed were investigated numerically, and the primary results are summarized in graphical and tabular form.

I. INTRODUCTION

The problem of selecting a design storm upon which to base detailed computations of storm tide requires a knowledge of how different storms will affect the water level for the location concerned. One can certainly gain some idea of the water level response from empirical data. However for any single location, the number of situations involving storm tides of hurricane proportions is definitely limited, and the information is usually not sufficient for the selection of those storm conditions which will be most severe. The New England area is a case in point. Moreover, if one examines the water level data from several different locations for the same storm, it is difficult to separate the direct effects of the storm from the special influences of the local topographic conditions in the vicinity of the different tide recording stations.

The alternative is to look to the hydrodynamic equations governing the generation of the storm surges. The exact equations are so complicated that a complete mathematical solution, capable of dealing with any storm condition, is outside the realm of practicality. Yet we need numerical results for a wide variety of storm conditions in order to make it possible to select the most severe.

Obviously a compromise is necessary. A number of different special theories for the generation of storm surges exist in the literature. However very few of these seem to be applicable to the New England situation. Most of the special theories deal with water of constant depth. An exception is the edge-wave theory. However the latter is difficult to

apply for a large variety of storm conditions. In fact the labor involved in the determination of numerical results from most of the existing special theories makes their use practically prohibitive. The use of a storm tide potential such as that suggested in a previous technical report (Reid and Wilson, 1955, pp. 5-7) takes bottom slope into account but is evidently applicable only for quasi-stationary storms, since it is based essentially upon the static set-up equation. What is needed is a rapid method for evaluating the approximate storm tide which will take into account bottom slope and dynamic effects related to the movement of the storm. The method must be rapid enough that a large number of cases can be evaluated. Different combinations of fetch lengths (storm size) and storm speeds, as well as different wind and pressure distributions need to be investigated. The prime requirement of the method is that it lead to calculated storm tides which are in reasonable accord with observations. The advantage over purely empirical findings being that the definition of a complete response diagram is possible.

In the present report an approximate procedure for the evaluation of storm tide is outlined. This is based upon the simplified, linear, one-dimensional equations of motion, and utilizes the method of characteristics as the tool for solution. The numerical results are obtained essentially by a simple graphical integration procedure. This procedure takes bottom slope into account, and is capable of dealing with most any distribution of onshore components of wind speed or atmospheric pressure. In the analysis to date only the wind-driven surges have been examined. Furthermore, in order to facilitate the interpretation of the results, the shape of the wind stress distribution was the same in all cases. However, different combinations of the fetch length and speed of propagation of the storm were examined. Furthermore the effect of the wind intensity is readily taken into account by employing a dimensionless form of the basic equations.

The results of computations for the approximate storm tide at shore, for a bottom topography approximating that of the continental shelf off Narragansett Bay, are presented in the form of a response diagram. This gives the estimated maximum water level associated with a storm of a given maximum wind speed, fetch length, and speed of propagation. In all cases the storm is considered to be moving directly towards shore (path perpendicular to the shore). Some sample curves of the variation of computed water level with time are presented for comparison with observations. In addition some further refinements of the method are indicated.

The resulting estimates of water level by the present approximate theory are not considered sufficiently accurate for use in design calculations, since various effects such as those related to finite storm width, dissipation of energy by bottom friction, and local topographic irregularities are not considered. However the response diagram

from the present development does give a rational criterion upon which the selection of the design storm can be based. The predictions of water level from the response diagram presented in this report should therefore be referred to more appropriately as the "dynamic storm-tide potential". Values of this potential have been computed for the hurricanes of September, 1938, September, 1944, and August, 1954 (Carol).

II. METHOD OF CHARACTERISTICS

1. The Presumed Equations of Motion.

The following linearized differential equations of motion and continuity are taken as the starting point in the simplified one-dimensional water level problem:

$$(1) \quad \frac{\partial Q}{\partial t} + gh \frac{\partial \eta}{\partial x} = \left[\frac{\tau}{\rho} - \frac{h}{\rho} \frac{\partial p_a}{\partial x} \right]$$

$$(2) \quad \frac{\partial \eta}{\partial t} + \frac{\partial Q}{\partial x} = 0$$

where x is the horizontal coordinate taken normal to shore, t is time, g the acceleration of gravity, ρ the density of sea water, and h is the mean depth of water at position x . The quantities τ and p are considered as prescribed functions of x and t , representing respectively the wind stress in the x direction and the sea level atmospheric pressure. The quantities η and Q are the basic unknown functions of x and t , representing respectively the anomaly of water level above the predicted astronomical tide and the volume transport in the x direction through a vertical section of depth h and unit width transverse to the x -axis. The mean current associated with the forced surge at position x and time t is simply Q/h .

These equations represent an obvious simplification of the real problem, since two-dimensional effects associated with finite storm width, longshore winds, and variation of bottom topography parallel to shore are not considered. Furthermore bottom friction and non-linearity, associated with large water level changes, are not included. However for storms of large width parallel to shore and for conditions wherein η is smaller than h , the above equations can lead to reasonably realistic results.

2. Bottom Topography.

The mean bottom topography of the continental shelf in the vicinity of Narragansett Bay can be approximated by a uniform slope out to about 84 nautical miles from the mouth of the Bay. The depths along four equally spaced N-S lines between Montauk Point and Martha's Vineyard are

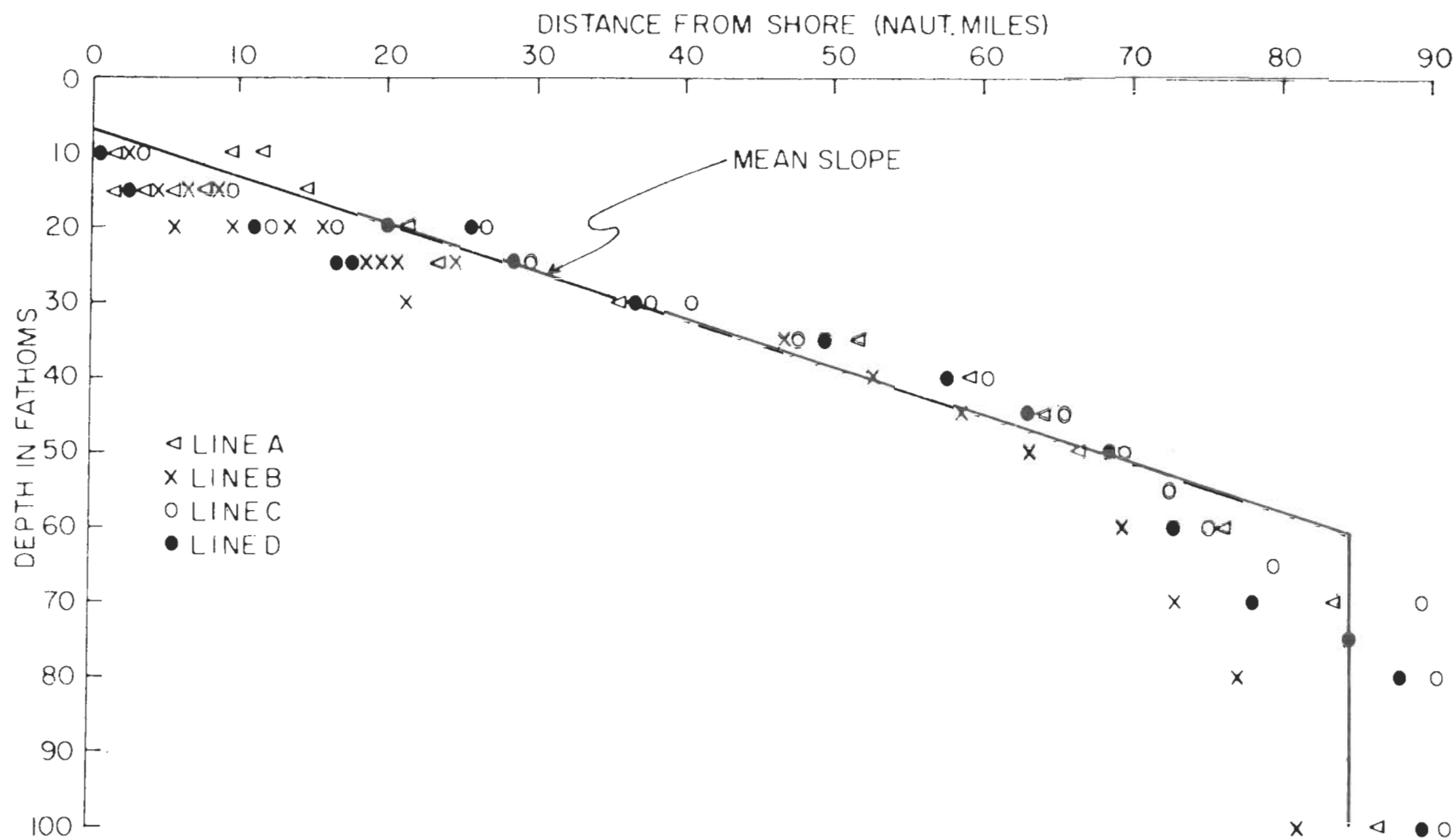


FIGURE 1 • MEAN BOTTOM PROFILE OFF NARRAGANSETT BAY

plotted in Figure 1. The slope near shore and at the edge of the shelf is so much steeper than that of the continental shelf that for practical purposes the bottom topography can be approximated by the full line which has been fitted to the points. For convenience in the mathematical development, the zero reference for x is taken inland from the coast such that

$$(3) \quad h = mx \quad \text{for} \quad x_0 \leq x \leq x_1,$$

where x_0 is the mean position of the shore line and x_1 is that of the edge of the shelf. The effective depth at shore will be denoted by h_0 and that at the edge of the shelf by h_1 . The width of the shelf ($x_1 - x_0$) will be denoted by L . For the present case the appropriate values are

$$\begin{aligned} h_0 &= 36 \text{ feet} & m &= 1/1580 \\ h_1 &= 360 \text{ feet} & x_0 &= 9.33 \text{ nautical miles} \\ L &= 84 \text{ nautical miles} & x_1 &= 93.3 \text{ nautical miles} \end{aligned}$$

and

$$x_0/x_1 = h_0/h_1 = 1/10$$

3. Transformation of the differential equations.

It is convenient to introduce the following dimensionless variables

$$(4) \quad \left\{ \begin{array}{ll} \text{(i)} & y = \sqrt{x/x_1} \\ \text{(ii)} & t' = t/T \\ \text{(iii)} & Z = \frac{\eta C_1 \sqrt{y}}{U^2 T} \\ \text{(iv)} & Y = \frac{Q}{U^2 T \sqrt{y}} \\ \text{(v)} & f = \frac{-1}{U^2} \left[\frac{\tau}{\rho} - \frac{h}{\rho} \frac{\partial p_a}{\partial x} \right] \quad (f > 0: \text{ onshore stress}) \\ \text{(vi)} & \gamma = 1 - \sqrt{h_0/h_1} \end{array} \right.$$

where

$$(5) \quad \left\{ \begin{array}{ll} (i) & T = L/\bar{C} \\ (ii) & C_0 = \sqrt{gh_0} \\ (iii) & C_1 = \sqrt{gh_1} \\ (iv) & \bar{C} = \frac{1}{2}(C_0 + C_1) \end{array} \right.$$

The quantity \sqrt{gh} represents the velocity of progress of free, long waves for a depth h . The quantity T is simply the travel time for a free, long wave to cross the shelf, i.e.,

$$(6) \quad T = \int_{x_0}^{x_1} \frac{1}{\sqrt{gh}} dx$$

where h is taken as mx . The quantity U has the dimensions of velocity and can be selected such that the maximum value of f is unity for convenience in analysis. Thus U^2 represents the maximum absolute value (or amplitude) of the driving force term in brackets on the right hand side of equation (1).

By taking $h = mx$ and making use of the transformations of equations (4i) to (4vi) it can be shown that equations (1) and (2) are rendered in the form:

$$(7) \quad \frac{\partial Y}{\partial t} + \gamma \left[\frac{\partial Z}{\partial y} - \frac{1}{2} \frac{Z}{y} \right] = -y^{-1/2} f$$

$$(8) \quad \frac{\partial Z}{\partial t} + \gamma \left[\frac{\partial Y}{\partial y} + \frac{1}{2} \frac{Y}{y} \right] = 0$$

The functions Y and Z which satisfy these equations will be referred to hereafter as the "exact" solutions. It is possible to evaluate exact solutions for a few limiting cases. For example if the driving force f is identically zero then the exact solutions for Y and Z can be expressed respectively in terms of Bessel functions of zero order and first order in the argument y ; and the time dependency is simple harmonic. Such solutions represent shelf seiche phenomena of simple one-dimensional type. As a second example the situation of steady state response to a sustained uniform driving force leads to a simple exact solution for Z involving the logarithm of y .

In the general case where f is neither uniform nor steady, the exact solution of equations (1) and (2) is extremely complicated. To facilitate the solution in order that a wide variety of forcing functions can be dealt with, a method of successive approximations can be used. In the present report we will be concerned primarily with the first approximation for Y and Z . We obtain such an approximation by dropping the terms Z/y and Y/y compared with $\partial Z / \partial y$ and $\partial Y / \partial y$ respectively in equations (1) and (2). In the case of free seiche motion ($f = 0$) this implies that space dependency of Y and Z is expressible in terms of \sin and \cos functions involving the argument y . In fact the first approximation solutions are simply the asymptotic forms of the exact Bessel function solutions of equations (1) and (2), which apply if y_0 is sufficiently large. This implies that if the quantity $\sqrt{h_0 h_1}$ is not too small then the first approximation solution is not too greatly different from the exact solution. Later in the report, accuracy of the first approximation is examined for two special cases.

4. The Method of Characteristics Applied* to the First Approximation Equations.

The first approximations for Y and Z are those functions satisfying the equations

$$(9) \quad \frac{\partial Y}{\partial t'} + \gamma \frac{\partial Z}{\partial y} = -y^{-1/2} f$$

$$(10) \quad \frac{\partial Z}{\partial t'} + \gamma \frac{\partial Y}{\partial y} = 0$$

The sum of equations (9) and (10) gives

$$(11) \quad \frac{\partial}{\partial t'} (Y + Z) + \gamma \frac{\partial}{\partial y} (Y + Z) = -y^{-1/2} f$$

while the difference of (9) and (10) yields

$$(12) \quad \frac{\partial}{\partial t'} (Y - Z) - \gamma \frac{\partial}{\partial y} (Y - Z) = -y^{-1/2} f$$

Equations (11) and (12) can be written in a more usable form as follows:

$$(13) \quad \frac{d}{dt'} (Y + Z) = -y^{-1/2} f, \quad \text{for } \frac{dy}{dt'} = \gamma$$

$$(14) \quad \frac{d}{dt'} (Y - Z) = -y^{-1/2} f, \quad \text{for } \frac{dy}{dt'} = -\gamma$$

* For a general discussion of the method of characteristics and its application see for example Freeman (1951).

A path in the y, t' plane having the slope $\pm \gamma$ is called a characteristic curve and the values of $Y \pm Z$ along such lines are governed by the forcing function and initial or boundary conditions. Those characteristics whose slope is positive are referred to as the positive characteristics, while those with negative slope are referred to as negative characteristics.

Free Waves: In the case of free waves ($f = 0$), equations (13) and (14) imply that

$$(15) \quad Y + Z = \text{constant, along } \frac{dy}{dt'} = \gamma$$

$$(16) \quad Y - Z = \text{constant, along } \frac{dy}{dt'} = -\gamma$$

Consider any positive characteristic A which passes out of the shaded region from point P_0 in Figure 2-A. If we assume that the water is initially undisturbed and at rest between 0 and E then Y and Z must be zero along the y axis up to point E. Consequently from equation (15),

$$(17) \quad Y + Z = 0 \text{ along } A.$$

Now consider a negative characteristic which emanates from point P_1 in the region offshore where a disturbance exists (Y_1 and Z_1 not zero). At the intersection point P, we must have $Y = -Z$ by equation (17). Consequently equation (16) yields

$$(18) \quad 2Z = (Z_1 - Y_1).$$

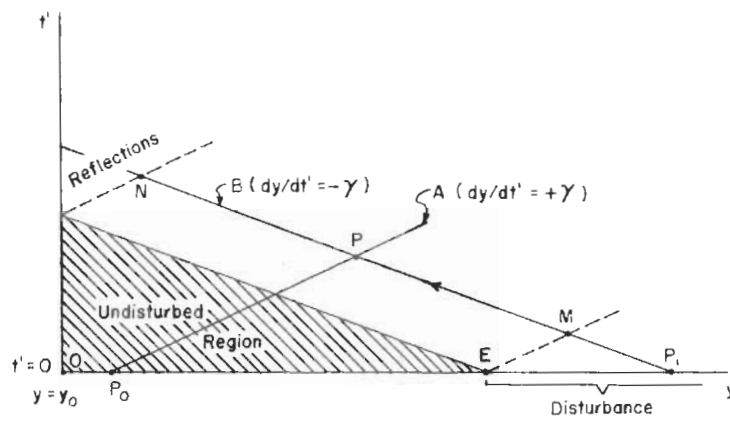
This holds for any point P on the characteristic B between the two dashed characteristics lines. Consequently

$$(19) \quad Z = \text{constant along } B \text{ from } M \text{ to } N,$$

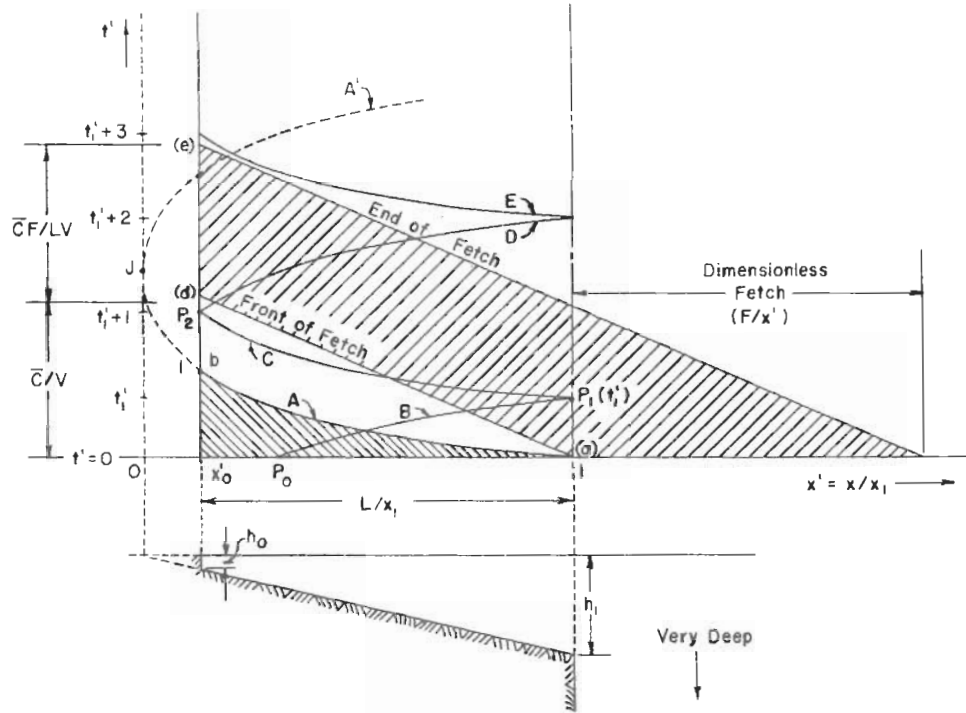
for a free disturbance. If we consider that point P_1 represents the crest of the disturbance (wave) at $t = 0$, then its position at any other time will be determined by the characteristic line B. The value of Z remains constant along this line, but in view of eq. (4iii)* η will vary as $y^{-1/2}$ and hence the height of the free wave will increase towards shore like $h^{-1/4}$. This result is consistent with Green's law (Lamb, 1945, pp. 274-5) for the amplification of a free disturbance of long wave length on a gradually sloping shelf, and can be derived independently from energy considerations.

To the left of point N, assuming that a sea wall exists at the position y_0 , reflection will occur and the free wave is therefore modified.

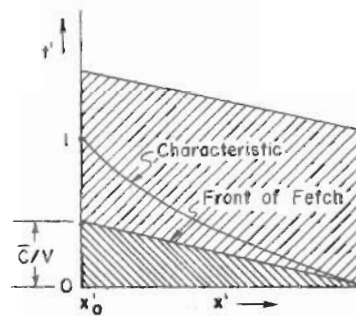
* In the case of free waves U must be regarded as some arbitrary constant different from zero.



A. Free Wave



B. Forced Wave ($V < \bar{C}$)



C. Forced Wave ($V > \bar{C}$)

FIGURE 2 · SCHEMATIC CHARACTERISTIC DIAGRAMS

Forced Waves: The special case of free waves was discussed primarily for the purpose of demonstrating that the method of solution as applied to the first approximation equations does lead to a commonly accepted relationship. In the case of forced waves the situation is not nearly as simple, however the method of characteristics still allows a direct approach.

Consider now the x' , t' -diagram ($x' = x/x_1$) shown in the upper part of Figure 2-B. The selected bottom profile is shown in the lower diagram. In the x' , t' -diagram the characteristic lines are parabolas with a vertex at the position $x' = 0$ (see line A-A', vertex at point J). This can be seen from the relation

$$(20) \quad \frac{dy}{dt'} = \pm \gamma$$

which upon integration and using equation (4i) yields

$$(21) \quad \sqrt{x'} = \pm \gamma t' + \text{const}$$

The travel time of a free wave across the shelf is T ; consequently the value of $\Delta t'$ from (a) to (b) along characteristic A is unity. This determines the characteristic curves uniquely. The change in slope of the characteristics on the x' , t' -diagram is related to the change of the wave speed \sqrt{gh} .* The curved characteristic lines in the x' , t' -diagram are simply transformations of the straight characteristic lines in the y , t' -diagram. The x' , t' -diagram is more convenient in respect to plotting the wind field for a storm which travels at constant velocity.

Suppose a storm with finite fetch is moving at constant velocity V across the shelf (upper shaded area Fig. 2-B). The time origin is taken such that the beginning of the fetch is located at the edge of the shelf at $t = 0$ as shown. Outside of the fetch area the value of f is considered negligible. Thus at $t = 0$ we can consider that the values of Y and Z are zero (hydrostatic equilibrium). The first disturbance (of negligible magnitude) will be propagated along the characteristic A, so that if $V < \bar{C}$ (as is the case shown in Fig. 2-B) then there will be no disturbance within the lower shaded area. The reverse situation is shown in Fig. 2-C. In this case $V > \bar{C}$ so that the region of no disturbance on the x' , t' -diagram is now delineated by the x' -axis and the beginning of the fetch area.

Returning now to Fig. 2-B, it should be pointed out that a disturbance created at the edge of the shelf ($x' = 1$) will arrive prior to the beginning of the fetch at other positions on the shelf since for this case $\bar{C} > V$. Thus the water level at shore will start to change before the storm arrives, if the latter is traveling slower than the average free-wave velocity on the shelf.

* Note that since the t' axis is along the ordinate, large slopes represent small velocity and vice versa.

If the storm is not moving with constant velocity across the shelf then the leading edge (and end) of the fetch will appear as curved lines on the x', t' -diagram. Furthermore isolines of f can be constructed within the fetch area to give a quantitative description of the force field.

5. Boundary Conditions.

Before we can embark on a discussion of the method of determining the water level at shore it is necessary to choose suitable boundary conditions at shore and at the edge of the shelf. The conditions utilized in most of the calculations summarized in the latter part of the report are as follows:

$$(22) \quad \begin{cases} (i) & Z = 0 \quad \text{at} \quad x = x_1 \quad (\text{edge of shelf}) \\ (ii) & Y = 0 \quad \text{at} \quad x = x_0 \quad (\text{shore}) \end{cases}$$

The first of these is valid only if p_a is uniform and if the depth of the ocean beyond the edge of the shelf is sufficiently deep such that the wind stress has negligible effect for $x' > 1$. The second condition stipulates that no flow of water occurs across the shoreline. Both of these conditions are obviously approximations, but are probably consistent with other approximations in the present theory. More realistic conditions can be utilized; (one such modification for the edge of the shelf is discussed in a later section). However the above conditions are considered adequate for the present analysis of the approximate water level response.

6. Determination of the Forced Water Level at Shore.

Returning to equation (13) it can be seen that along the positive characteristic B of Fig 2-B

$$(23) \quad Y + Z = - \int_0^{t'} (y^{-1/2} f)_B \, dt' + Y_0 + Z_0$$

where the integration is carried out with respect to t' along the line B. Now $Y_0 = Z_0 = 0$, so that at point P_1 (time t_1'), the value of Y is given by

$$(24) \quad Y_1 = - \int_0^{t_1'} (y^{-1/2} f)_B \, dt'$$

since $Z_1 = 0$ by boundary condition (22i). For the negative characteristic C we have from equation (14)

$$(25) \quad Y - Z = - \int_{t_1'}^{t'} (y^{-1/2} f)_C dt' + Y_1 - Z_1$$

where the integration is carried out with respect to t' along the line C. At point P_2 (time $t_1' + 1$) we have for the value of Z at shore

$$(26) \quad Z(x_0', t_1' + 1) = \int_{t_1'}^{t_1' + 1} (y^{-1/2} f)_C dt' - Y_1$$

since Y_2 and Z_1 are zero according to the boundary conditions. Combining equations (24) and (26) yields:

$$(27) \quad Z(x_0', t_1' + 1) = \int_0^{t_1'} (y^{-1/2} f)_B dt' + \int_{t_1'}^{t_1' + 1} (y^{-1/2} f)_C dt'$$

If the same procedure is carried up to time $t_1' + 3$ along characteristics D and E (Fig. 2-B) we find at the shore:

$$(28) \quad Z(x_0', t_1' + 3) = \int_{t_1' + 1}^{t_1' + 2} (y^{-1/2} f)_D dt' + \int_{t_1' + 2}^{t_1' + 3} (y^{-1/2} f)_E dt' - Z(x_0', t_1' + 1)$$

For the special case of Fig. 2-B, the second integral in equation (28) vanishes since the characteristic E lies wholly outside of the fetch area on the x', t' -diagram.

If we proceed two more units of t' we find that at shore;

$$(29) \quad Z(x_0', t_1' + 5) = Z(x_0', t_1' + 3)$$

for the situation of Fig. 2-B. Again for two more time units

$$(30) \quad Z(x_0', t_1' + 7) = Z(x_0', t_1' + 3)$$

Now if t_1' is chosen as any value between zero and unity it is possible to evaluate $Z(x_0', t')$ for all t' by successive application of this method.

The values of $Z(x_0', t')$ for the situation of Fig. 2-B will proceed from zero at time $t' = 1$ to a maximum (assuming f positive) somewhere between times d and e , and for $t' > e$, the water level will oscillate as a seiche with period $\Delta t' = 4(\Delta t = 4T)$. It is possible with just the right combination of fetch length and speed to have virtually no seiche after the storm has moved inshore. In other cases the seiche amplitude may be nearly the same as the first maximum attained during the passage of the storm. Later considerations disclose that the description of the seiche or resurgences by the present theory is less reliable than the estimation

of the first maximum. Furthermore the forced maximum water level is the highest. Consequently most of the attention has been focused upon the latter in the analysis work.

7. The Model Fetch.

In the present analysis p_a was considered uniform in the first approximation. The effect of non-uniform atmospheric pressure might be accounted for approximately by adding to the wind-induced water level a value equal to the deficit of pressure from normal (expressed as a head of water). Usually this will not amount to more than two feet, while the wind-induced head at shore can be as great as 10 to 15 feet. Of course the astronomical tide must be added to the wind-induced water level as well.

As a working model the forcing function was taken as

$$(31) \quad \begin{cases} f = 1 - \frac{2}{F} |x|, & \text{for } |x| \leq \frac{F}{2} \\ f = 0 & , \text{ for } |x| \geq \frac{F}{2} \end{cases}$$

where

$$(32) \quad X = x + vt - x_1 - \frac{F}{2},$$

F being the fetch length and V the shoreward velocity of the storm. This distribution is shown schematically in Fig. 3-A. The fetch length is shown in dimensionless form as F/x_1 , the half fetch length in dimensionless form being denoted by a_0 , thus

$$(33) \quad 2a_0 = \frac{F}{x_1}$$

We can rewrite equation (31) in the form

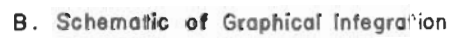
$$(31\text{-ii}) \quad \begin{cases} f = 1 - \left| \frac{a}{a_0} \right|, & \text{for } |a| \leq a_0 \\ f = 0 & , \text{ for } |a| \geq a_0 \end{cases}$$

where

$$(34) \quad a = x' + vt' - 1 - a_0$$

and

$$(35) \quad v = \frac{VT}{x_1} = \frac{L}{x_1} \frac{V}{C}$$



14

Since the gradient of p_a is neglected, the quantity $\rho U^2 f$ is simply the wind stress in the negative x -direction (towards shore). Thus U^2 is the maximum value of τ/ρ in the fetch. The working model for f (hence τ/ρ) is compared with the form of the wind stress distributions for three actual storms (Figs. 17, 18, and 19). These are discussed in a later section. It is sufficient to say at this point that the linear distribution of the shoreward component of wind stress seems reasonable, at least for the first three-quarters of the fetch.

8. Graphical Integration Technique.

The method of evaluation of the integrals in equations (27), (28) etc. is illustrated in Figure 3-B. For each α_0 investigated, a field of G , where

$$(36) \quad G = y^{-1/2} f,$$

was constructed. In all of these graphs the value of $x_0' (=h_0/h_1)$ was taken as 0.1 which applies to the New England shelf region (off Narragansett Bay). The isolines of G are spaced linearly along any ordinate but the peak values along the ridge line (dashed line in Fig. 3-B) vary as $y^{-1/2}$ or $(x/x_1)^{-1/4}$ from unity at $x' = 1$ to 1.78 at $x' = 0.1$.

Consider the characteristics B emanating from the lower shaded area and its reflected image C . According to equation (27) the value of Z at shore for point P is equal to the combined integrals with respect to time along the paths B, C . This integral is obtained as follows: the intersections of the isolines of G with the characteristic path are projected horizontally onto the auxiliary graph of G versus t' at the appropriate value of G . These projected points delineate a curve D , the area between this curve and the t' -axis being proportional to Z . If A is the area in square inches and M_1 and M_2 are the scale moduli in inches, for the t' and G scales respectively, then for point P

$$(37) \quad Z = \frac{A}{M_1 M_2}$$

In the calculations the areas were evaluated by use of a standard planimeter measuring directly in square inches. All areas were constructed on transparent overlays applied to the basic grid (given α_0). Different storm speeds were investigated by varying the modulus M_1 of the characteristic curve. A standard set of such curves were constructed as templates in order to facilitate the graphical work, and these could be applied for any basic grid. Values of v were determined for each case from the formula

$$(38) \quad v = \frac{0.9 M_1}{M_3} \quad \text{or} \quad \frac{v}{c} = \frac{M_1}{M_3}$$

where M_3 is the scale modulus for the basic grid (see Fig. 3-B). Sample plots of G and corresponding Z values for the case of $F = 2L$, $V = \bar{C}$ are given in Fig. 21.

A total of 55 different combinations of F/L and V/\bar{C} were investigated. Of these cases 27 were studied in detail in order to determine the entire history of Z at shore from its initial zero state up to the maximum and to the beginning of the seiche phenomenon. Each of these cases required about ten to fifteen graphical integrations of the type discussed above in order to define the curves adequately. In the remaining cases only three or four integrations were carried out in the general region of the maximum Z in order to define the value and time of occurrence of the latter.

Figure 4 shows the variation of Z at shore versus t' pertaining to five different fetch lengths* for the selected storm speed of $V = \bar{C}$ ($v = 0.9$). On this graph and hereafter in the report, the value of Z at shore is designated as Z_0 . The beginning of the seiche is shown for the cases $F/L = 0.5, 1.0$ and 2.0 . The time of passage of the front of the fetch at shore for all five cases in Fig. 4 is $t' = 1$, since for these cases $V = \bar{C}$. The times of passage of the end of the fetch (t_e') at shore are

$F/L:$	0.50	1.0	2.0	4.0	8.0
$t_e':$	1.50	2.0	3.0	5.0	9.0

The time (t_m') of maximum Z_0 and the time (t_w') of passage of the maximum wind are listed below for these same cases.

$F/L:$	0.5	1.0	2.0	4.0	8.0
$t_m':$	1.25	1.6	2.1	3.1	5.0
$t_w':$	1.25	1.5	2.0	3.0	5.0

Thus for these cases the maximum Z_0 occurs near the time of maximum wind at shore. The particular case of $F/L = 4.0$, $V/\bar{C} = 1$ gives a maximum Z_0 of 1.84 which is the highest for all of the 55 cases investigated.

Figure 5 shows the time variation of Z_0 associated with eight different values V/\bar{C} . The fetch length in all of these cases is the same $F = 0.5L$ ($2\alpha_0 = 0.45$). The curves for $V/\bar{C} = 0.2$ and 0.16 show the seiche phenomena clearly. The situation for small values of V/\bar{C} looks rather curious in that the maximum do not descend uniformly with decreasing V/\bar{C} as might be anticipated. The phenomenon is evidently not a result of errors in calculation since the same effect occurs for other fetch lengths, and appears to be related to the shape of the f distribution selected for the present study.

* The relative fetches F/L are indicated on the figure rather than α_0 . For the shelf off Narragansett Bay L is about 84 nautical miles. It will be recalled also that $t'' = t/T$ and T is about 2 hours.

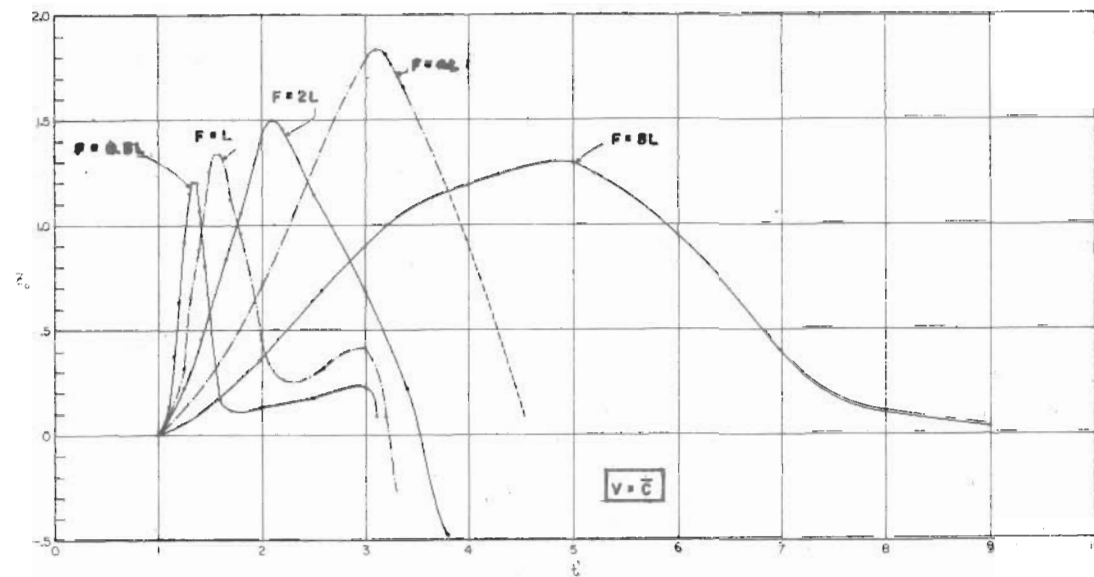


FIGURE 4 · Z_0 VERSUS t' FOR $V = \bar{c}$ AND VARIOUS F/L

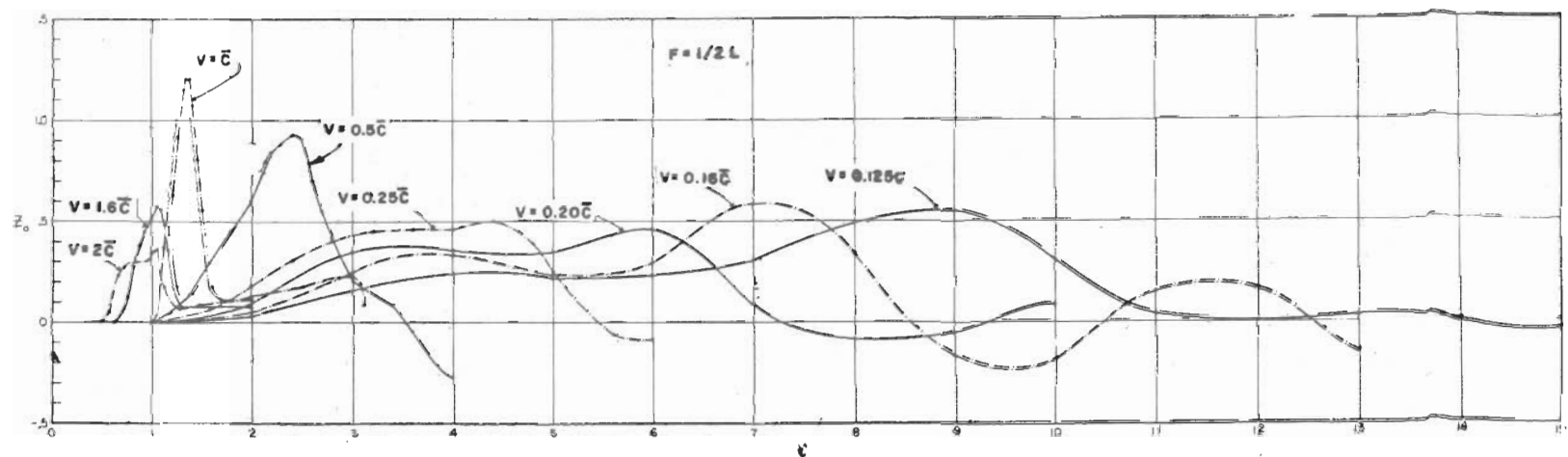


FIGURE 5 · Z VERSUS t' FOR $F = L/2$ AND VARIOUS V/\bar{c}

III. LIMITING CASES

1. Steady State.

The method of characteristics as applied to the case of small v requires a great many graphical integrations and therefore becomes impractical. The limiting case of $v = 0$ can be analysed by a different procedure using the steady state differential equations, and serves as a useful control. Furthermore this is one case for which the exact solution is easily determined.

Returning to equations (7) and (8) we have for the special case of steady state

$$(39) \quad \gamma \left(\frac{\partial Z}{\partial y} - \frac{1}{2} \frac{Z}{y} \right) = -y^{-1/2} f$$

and Y must be zero in order to satisfy equations (8) and (22ii). For the first approximation, equation (39) reduces to

$$(40) \quad \gamma \frac{dZ}{dy} = -y^{-1/2} f \quad (1st \text{ approx.})$$

while for the exact case we can write (39) in the form

$$(41) \quad \gamma \frac{\partial}{\partial y} (y^{-1/2} Z) = -y^{-1} f \quad (\text{Exact})$$

The solutions are respectively:

$$(42) \quad Z_0 = \frac{1}{\gamma} \int_{y_0}^1 y^{-1/2} f dy \quad (1st \text{ approx.})$$

$$(43) \quad Z_0 = \frac{1}{\gamma} y_0^{1/2} \int_{y_0}^1 y^{-1} f dy \quad (\text{Exact})$$

Values of Z_0 for different positions of the fetch were determined from both equations, by numerical integration. This was done for six different values of α_0 . The maximum values of Z_0 for each of these cases are plotted in Fig. 6 (all values apply for $h_0/h_1 = 0.1$). The notation Z_m is used to denote the maximum value of Z at shore.

In the limiting case of very small α_0 the maximum Z_0 is obtained by taking $y \doteq y_0$ and

$$(44) \quad \int f dy \doteq \frac{1}{2y_0} \int f dx'$$

The maximum value of the integral on the right is simply α_0 so that equations

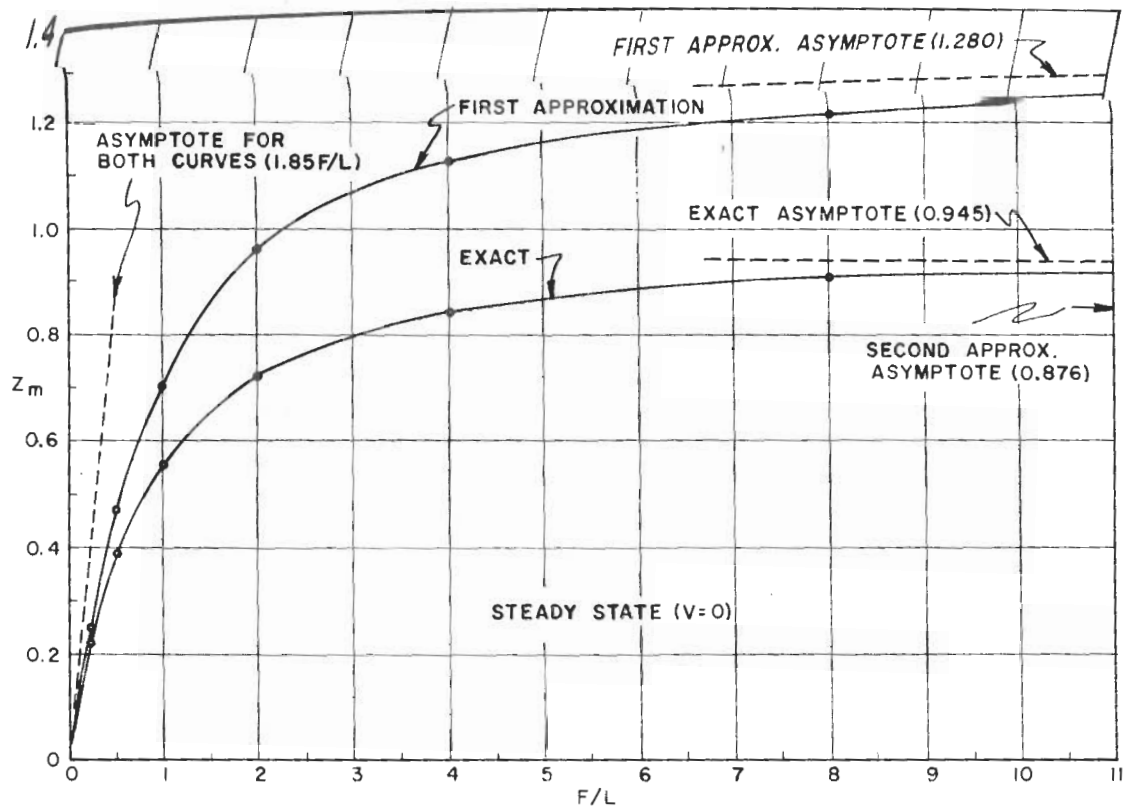


FIGURE 6 STEADY STATE Z_m VERSUS F/L , FIRST APPROXIMATION AND EXACT SOLUTION

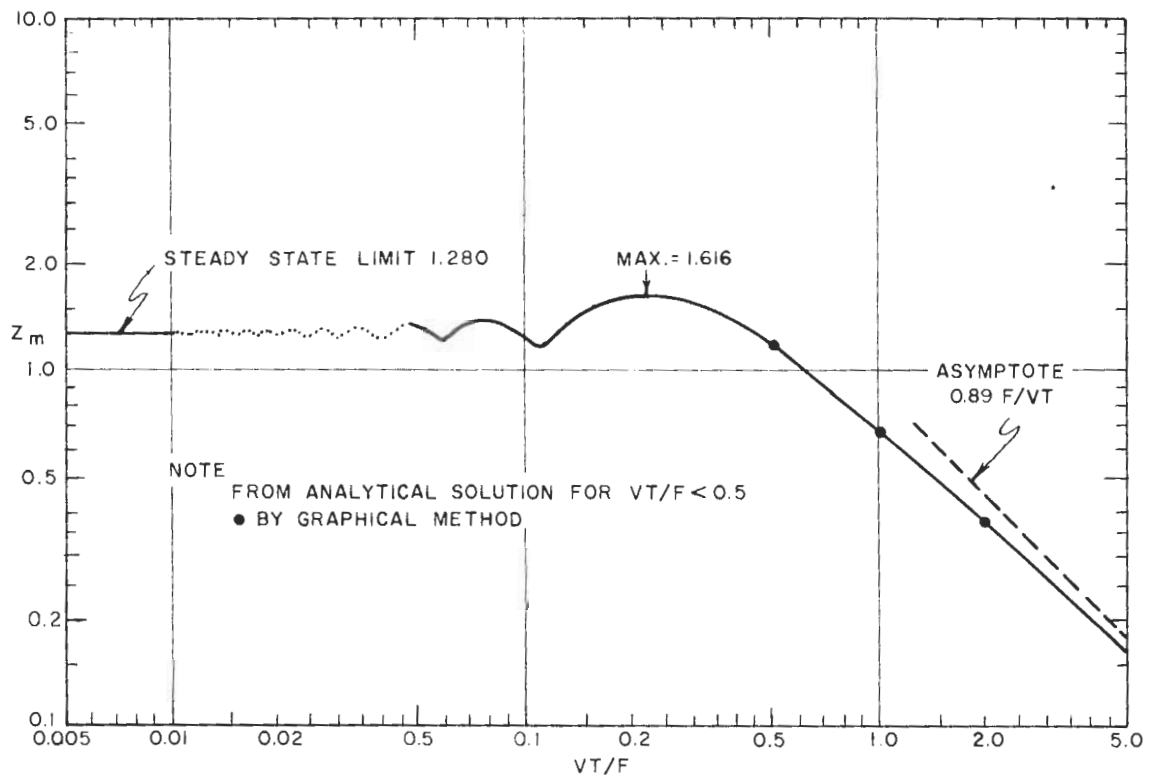


FIGURE 7 Z_m (FIRST APPROXIMATION) VERSUS VT/F FOR A UNIFORM WIND FIELD

(42) and (43) both lead to

$$(45) \quad Z_m = \frac{a_0}{2\gamma} \left(\frac{h_1}{h_0} \right)^{3/4}$$

for very small a_0 . This relation is shown as the asymptote through the origin in Fig. 6.

For the limiting case of very large a_0 , the forcing field can be considered uniform ($f = 1$), and equations (42) and (43) lead to

$$(46) \quad Z_m = \frac{2}{\gamma} (1 - y_0^{1/2}) \quad (\text{1st approx.})$$

$$(47) \quad Z_m = \frac{1}{\gamma} y_0^{1/2} \ln \frac{1}{y_0} \quad (\text{Exact})$$

The appropriate limiting values of Z_m for $h_0/h_1 = 0.1$ are 1.280 and 0.945 respectively.

The maximum difference between the first approximation and exact solutions for the steady state case is 0.335 or about 26 per cent of the first approximation. In the calculation of the final response curves, adjustments are applied to the first approximation values of Z on the basis of the steady state curves of Fig. 6. This is the primary use of the steady state solutions.

2. Uniform Wind Field.

The limiting case of a spacially uniform wind field which varies with time serves as a useful guide for the case of large fetch. The situation of spacially uniform f should lead to an asymptotic solution of the general problem (as $a_0 \rightarrow \infty$) if the time variation of f is selected as follows:

$$(48) \quad \begin{cases} \text{(i)} & f = \frac{vt'}{a_0}, \quad \text{for } 0 < t' < \frac{a_0}{v} \\ \text{(ii)} & f = 2 - \frac{vt'}{a_0}, \quad \text{for } \frac{a_0}{v} < t' < \frac{2a_0}{v} \\ \text{(iii)} & f = 0, \quad \text{for } t' > \frac{2a_0}{v} \end{cases}$$

The following solution for Z satisfies the first approximation equations (9) and (10) and the boundary condition (22):

$$(49) \quad Z = \sum_{n=1}^{\infty} \left[A_n \cos \left(\frac{2n-1}{2} \pi t' \right) + B_n \sin \left(\frac{2n-1}{2} \pi t' \right) + \frac{2k_n}{(2n-1)\pi} f(t') \right] \cos \left[\frac{2n-1}{2} \pi \frac{(y-y_0)}{\gamma} \right]$$

where

$$(50) \quad k_n = \frac{2}{\gamma} \int_{y_0}^1 y^{-1/2} \sin \left[\frac{2n-1}{2} \pi \frac{(y-y_0)}{\gamma} \right] dy$$

The values of A_n and B_n depend upon a_0/v and k_n and are given by different expressions for different time intervals as follows:

Time interval		A_n	B_n
(51) {	(i) $0 < t' < \frac{a_0}{v}$	0	$-P_n$
	(ii) $\frac{a_0}{v} < t' < \frac{2a_0}{v}$	$-2P_n \sin \beta_n$	$P_n (2 \cos \beta_n - 1)$
	(iii) $t' > \frac{2a_0}{v}$	$-2P_n \sin \beta_n (1 - \cos \beta_n)$	$2P_n \cos \beta_n (1 - \cos \beta_n)$

where

$$(52) \quad \begin{cases} (i) & P_n = \frac{4k_n}{\pi^2 (2n-1)^2} \frac{v}{a_0} \\ (ii) & \beta_n = \frac{\pi}{2} (2n-1) \frac{a_0}{v} \end{cases}$$

The first three values of k_n as evaluated by numerical integration for $h_0/h_1 = 0.1$ are

n	k_n
1	1.4989
2	0.7207
3	0.4218

and for large n

$$(53) \quad k_n = \frac{4}{\pi} \frac{(h_1/h_0)^{1/4}}{(2n-1)} = \frac{2.27}{(2n-1)}$$

Furthermore it can be shown that

$$(54) \quad \sum_{n=1}^{\infty} \frac{2k_n}{\pi (2n-1)} = \frac{1}{\gamma} y_0^{1/2} \ln \frac{1}{y_0} = 1.280$$

for $h_0/h_1 = 0.1$.

For the case of $v/\alpha_0 \leq 1$ the time of maximum Z_0 can be evaluated approximately by considering only the first terms ($n=1$) of the sum in equation (49).

This leads to the relations

$$(55) \quad \left\{ \begin{array}{ll} \text{(i)} & \cos\left(\frac{\pi}{2} t'_m + \delta\right) = \frac{1}{\sqrt{5 - 4 \cos \frac{\pi}{2} \frac{\alpha_0}{v}}} \\ \text{(ii)} & \tan \delta = \frac{-2 \sin \frac{\pi}{2} \frac{\alpha_0}{v}}{\left[2 \left(\cos \frac{\pi}{2} \frac{\alpha_0}{v}\right) - 1\right]} \end{array} \right. \quad \begin{array}{l} \text{Note:} \\ \frac{v}{\alpha_0} = \frac{VT}{F} \end{array}$$

from which t'_m can be obtained. This was used in equation (49) to evaluate the approximate maximum value of Z at shore ($y = y_0$) for $v/\alpha_0 \leq 1$ ($VT/F = 1/2$). The terms involving A_n and B_n were summed over $n = 1, 2, 3$; while the term involving k_n was summed in complete form by equation (54). The resulting curve for Z_m is shown in Fig. 7, (page 19).

As a check, the value of Z_m was evaluated by the graphical method of characteristics at the point $VT/F = 0.5$. The resulting value checks that deduced from the analytical solution at this point. In the graphical procedure, the lines of zero G are taken parallel to the x' axis since f varies only with t . These lines are separated by the time interval $\Delta t' = F/VT$ (Fig. 3-C, page 14). The analytical solution is difficult to apply for $VT/F = 0.5$ and the remainder of the curve in Fig. 7 was therefore evaluated by means of the graphical solution. It can be shown readily from the method of characteristics that for large values of VT/F the maximum value of Z behaves approximately as

$$(56) \quad Z_m = \left(\frac{h_1}{h_0}\right)^{1/4} \frac{F}{2VT}$$

This is the asymptotic line shown on the right hand side of Fig. 7 (for $h_0/h_1 = 0.1$).

The striking feature in regard to the curve of Z_m is the set of secondary maxima which occur at the approximate positions

$$VT/F = .225/3, .225/5, .225/7, \dots$$

while the primary maximum occurs at $VT/F = .225$. A similar feature was also indicated in the graphical determinations for the case of $F/L = 0.5$.

IV. HIGHER ORDER APPROXIMATIONS

1. Equations for the Higher Order Approximations.

The bulk of the computations carried out in the present analysis are based upon the approximate equations (9) and (10), or their equivalents (13) and (14). These solutions represent only first approximations of the exact equations (7) and (8). In the special case of steady state ($v = 0$) we were able to get the exact solutions to compare with the first approximation solution. It is of interest now to consider higher order approximations of the Y and Z which satisfy (7) and (8) for the general situation of finite v and α_0 .

In order to be more explicit in respect to terminology, we will let Y' and Z' represent the solutions of equations (9) and (10) which satisfy the boundary conditions (22) and the initial conditions $Y' = Z' = 0$. Thus Y' and Z' are the first approximation solutions. The solutions of the exact equations (7) and (8) can be represented in the form:

$$(57) \quad \begin{cases} (i) & Y = Y' + Y'' \\ (ii) & Z = Z' + Z'' \end{cases}$$

where the correction terms Y'' and Z'' are presumably of second order compared with Y' and Z' respectively. If relations (57) are substituted into equations (7) and (8) we obtain

$$(58) \quad \frac{\partial Y'}{\partial t'} + \frac{\partial Y''}{\partial t'} + \gamma \frac{\partial Z'}{\partial y} + \gamma \frac{\partial Z''}{\partial y} - \frac{\gamma(Z' + Z'')}{2y} = -y^{1/2} f$$

$$(59) \quad \frac{\partial Z'}{\partial t'} + \frac{\partial Z''}{\partial t'} + \gamma \frac{\partial Y'}{\partial y} + \gamma \frac{\partial Y''}{\partial y} + \frac{\gamma(Y' + Y'')}{2y} = 0$$

However since Y' and Z' satisfy equations (9) and (10), the underlined terms in the above equations drop out. Furthermore if we neglect Z'' compared with Z' , and Y'' compared with Y' , in the last terms on the left, we obtain

$$(60) \quad \frac{\partial Y''}{\partial t'} + \gamma \frac{\partial Z''}{\partial y} = \frac{\gamma Z'}{2y}$$

$$(61) \quad \frac{\partial Z''}{\partial t'} + \gamma \frac{\partial Y''}{\partial y} = -\frac{\gamma}{2} \frac{Y'}{y}$$

These equations are similar to equations (9) and (10), where the first approximation solutions take the place of a driving force. The natural oscillations of Y'' and Z'' in the absence of Y' and Z' have a period of 4 units of t' , which is the same as that of Y' and Z' . Since the latter serve as driving forces for the correction terms, it is apparent that a resonant condition will exist if Y' and Z' contain a finite seiche of undamped amplitude. Therefore equations (60) and (61) will lead to realistic corrections for a limited range of t' only. As long as Y'' and

Z'' remain small compared with Y' and Z' up to the time of the first maximum in Z , the analysis for the correction terms will be of value since we are concerned mainly with the best determination of the maximum value of Z for a given situation.

Equations for a third order correction term can be determined in a manner similar to that of obtaining the second order equations. These are the same as (60) and (61) with Y'' and Z'' replaced by Y''' and Z''' and Y' and Z' replaced by Y'' and Z'' . The third order corrections determined from these equations are added to the first and second to get better estimates of Y and Z .

The boundary and initial conditions to be satisfied by the second and higher order correction terms are the same as those for the first approximation since we have taken $Y(0, t^*) = 0$, $Z(y_1, t^*) = 0$, $Y(y, 0) = 0$, and $Z(y, 0) = 0$.

2. Steady State.

In the case of steady state ($v = 0$) we do not encounter the difficulty mentioned above. The equations for the second approximation reduce to

$$(62) \quad \frac{\partial Z''}{\partial y} = \frac{1}{2} \frac{Z'}{y}$$

and Y'' must vanish in order that the boundary conditions be satisfied. This case is of interest since we have established the exact solution for Z in this case and it is therefore possible to see how much improvement is possible by evaluating the second order correction term to be added to Z' .

For the case of a steady uniform wind field ($\alpha_0 = \infty$, $v = 0$) the first approximation for Z is given by

$$(63) \quad Z' = \frac{2}{\gamma} (1 - y^{1/2}).$$

This reduces to equation (46) when $y = y_0$. If we use this in equation (62) we find

$$(64) \quad Z'' = \frac{1}{\gamma} \left[\ln y + 2(1 - y^{1/2}) \right]$$

which reduces to zero at $y = y_1 = 1$ as required by the boundary conditions. The third approximation can be established from the equation

$$(65) \quad \frac{\partial Z'''}{\partial y} = \frac{1}{2} \frac{Z''}{y}$$

which with equation (64) leads to

$$(66) \quad Z''' = \frac{1}{2\gamma} \left[\frac{1}{2} (\ln y)^2 - 2 \ln \frac{1}{y} + 4(\gamma - y^{1/2}) \right]$$

The values of the first, second, and third approximations at $y = y_0$ (shore) for the case of $h_0/h_1 = 0.1$ are tabulated below along with the exact value of Z at shore from equation (47):

$$\begin{aligned} Z_0' &= 1.280 \\ Z_0' + Z_0'' &= 0.876 \\ Z_0' + Z_0'' + Z_0''' &= 0.955 \\ Z_0 &= 0.945 \quad (\text{Exact}) \end{aligned}$$

These values are indicated in Fig. 6 also. It will be noted that the discrepancy from the exact value alternates in sign with each successive approximation. The error of 35.2 per cent in the first approximation is reduced to 7.5 per cent for the second and to about 1 per cent for the third. Thus the method of successive approximations does seem to converge rapidly for the case of steady state.

3. Second Approximation for the Case of $F = L$, $V = \bar{C}/2$.

One case for a moving fetch with finite fetch length has been investigated. The case of $F/L = 1.0$ and $V/\bar{C} = 0.5$ was selected for this purpose as typical of the New England hurricanes.

In order to obtain the second approximation it is necessary to evaluate the entire field of the first approximations Y' and Z' on the x' , t' -diagram. So far we have indicated the method of evaluating Y' and Z' at the boundaries only. For any point x' , t' in the field we can evaluate Y' and Z' from equations (13 and (14). The procedure is rather time consuming since it requires evaluation of integrals of $y^{-1/2}f$ along the characteristics for many different time intervals. The additions and subtractions of the deduced fields of $Y+Z$ and $Y-Z$ can be done graphically by use of transparent overlays, and the boundary values of Y and Z can be taken into account in a similar manner. A complete description of the procedure is beyond the scope of this report.

The results of the computations and sequence of graphical overlays for the case of $F/L = 1.0$ and $V/\bar{C} = 0.5$ are shown in Figs. 8 and 9. Contours of Z'' are shown in Fig. 8 and contours of Y' in Fig. 9. These fields are except for a factor of $y^{-1/2}$ or $y^{1/2}$, the relative fields of water level and flow. The wind fetch is indicated in these figures by the straight dashed lines. The computations are based upon $h_0/h_1 = 0.1$ and the boundary conditions specified earlier.

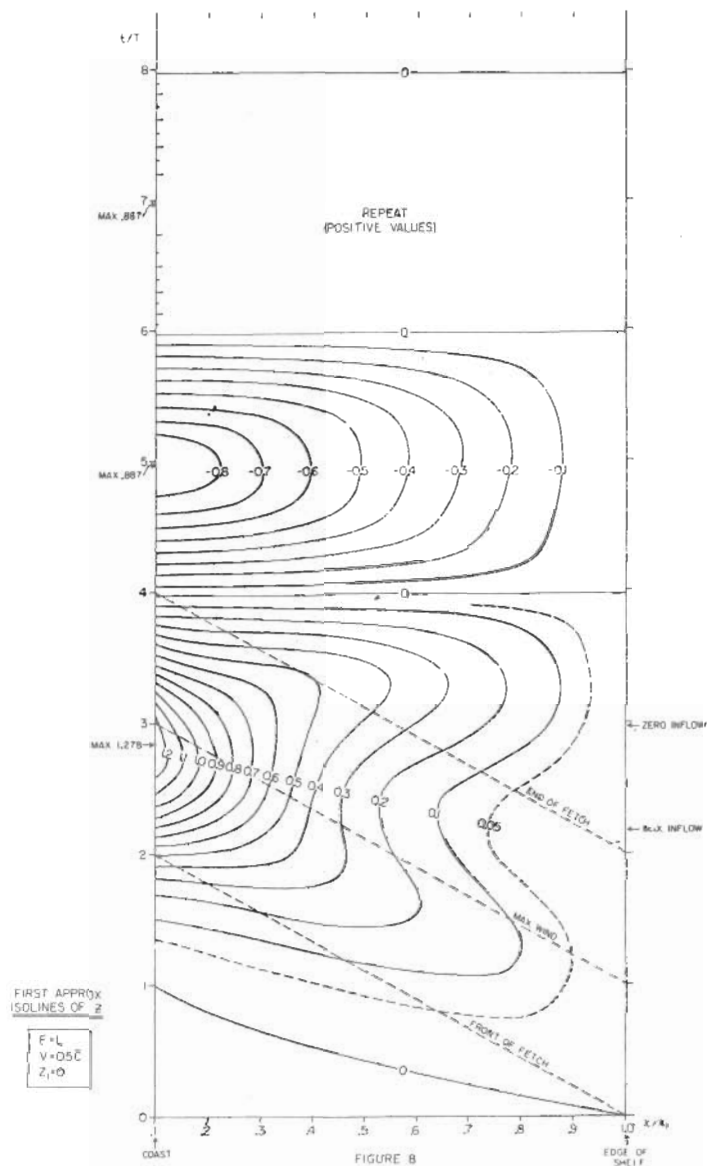


FIGURE 8 - FIELD OF FIRST APPROXIMATION VALUES OF Z FOR $V/\bar{C} = 0.5$, $F = L$

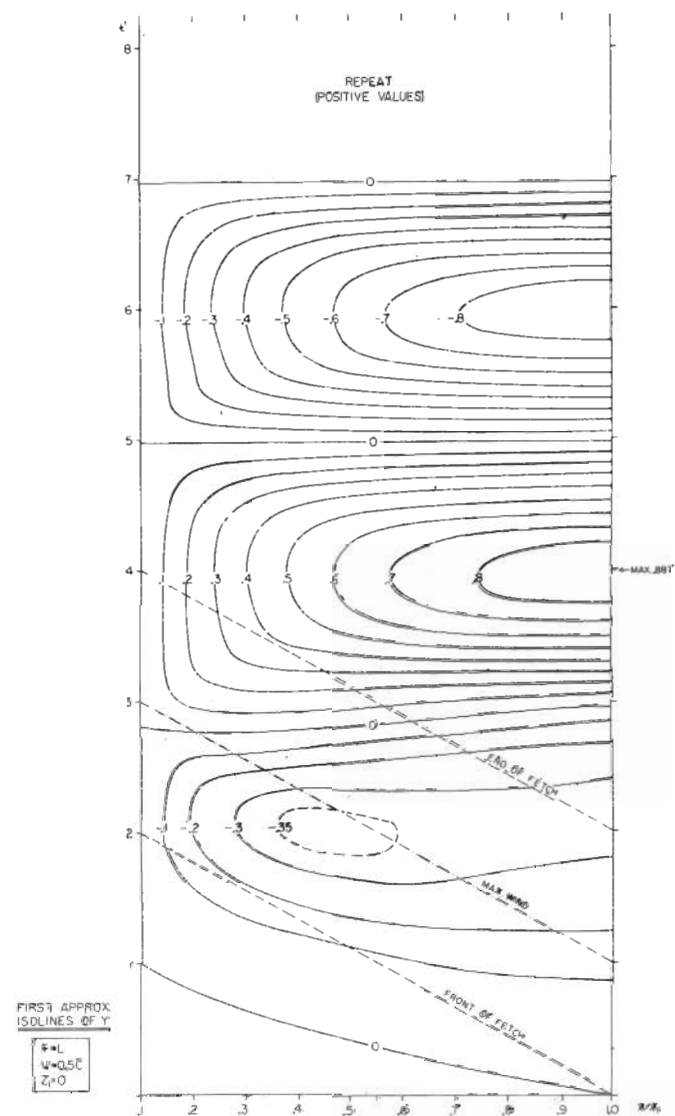


FIGURE 9 - FIELD OF FIRST APPROXIMATION VALUES OF Y FOR $V/\bar{C} = 0.5$, $F = L$

Profiles of the relative water level at successive time intervals for this case are shown in Fig. 15, the relative positions of the wind fetch also being indicated. Only the generation stage of the surge is reproduced in this figure. The relative water level was obtained from Z by multiplying the latter by $y^{-1/2}$, i.e., $(x/x_1)^{-1/4}$.

The second approximation of Z at shore can be determined from the equations

$$(67) \quad \frac{d}{dt'} (Y'' + Z'') = \frac{\gamma}{2y} (Z' - Y') \text{ along } \frac{dy}{dt'} = \gamma$$

$$(68) \quad \frac{d}{dt'} (Y'' - Z'') = \frac{\gamma}{2y} (Z' + Y') \text{ along } \frac{dy}{dt'} = -\gamma$$

which come directly from equations (60) and (61). These equations differ from the form of (13) and (14) in that the terms on the right side of equations (67) and (68) are different. Consequently in order to determine Z_0'' , two "force" fields must be constructed from the Y' and Z' fields. The procedure of evaluating Z_0'' is similar to that discussed in Section II-5 except that the integration along the positive and negative characteristics pertains to different "force" fields. Again the details of these computations are beyond the scope of this report. The results of the graphical integrations for Z_0'' , based upon the fields of Z' and Y' given in Figs. 8 and 9, leads to the dashed curve in Fig. 10. This is the sum of Z_0' and Z_0'' , i.e., the second approximation for Z_0 . The first approximation is also shown for comparison.

As indicated earlier, the method of successive approximation breaks down if carried over too large a range of t' since eventually the required condition that $Z'' \ll Z'$ is transcended. However at the position of the peak, the value of Z_0'' is of the order of 30 per cent of Z_0' and hence the second approximation is probably better than the first, up to the time of the maximum. The exact value of the maximum Z_0 probably lies between the two peaks indicated, but closer to that of the dashed curve.

The important thing shown by this analysis is that the resulting second order correction for Z in the case of a moving fetch is of the same order of magnitude and the same sign as that for the steady state case for corresponding Q_0 .

4. Modified Condition at the Edge of the Shelf.

If the depth of the ocean is considered of finite depth (h_2) beyond the shelf's edge, then it is possible for a surge of finite height to be transmitted beyond the shelf's edge after reflection from shore. If we

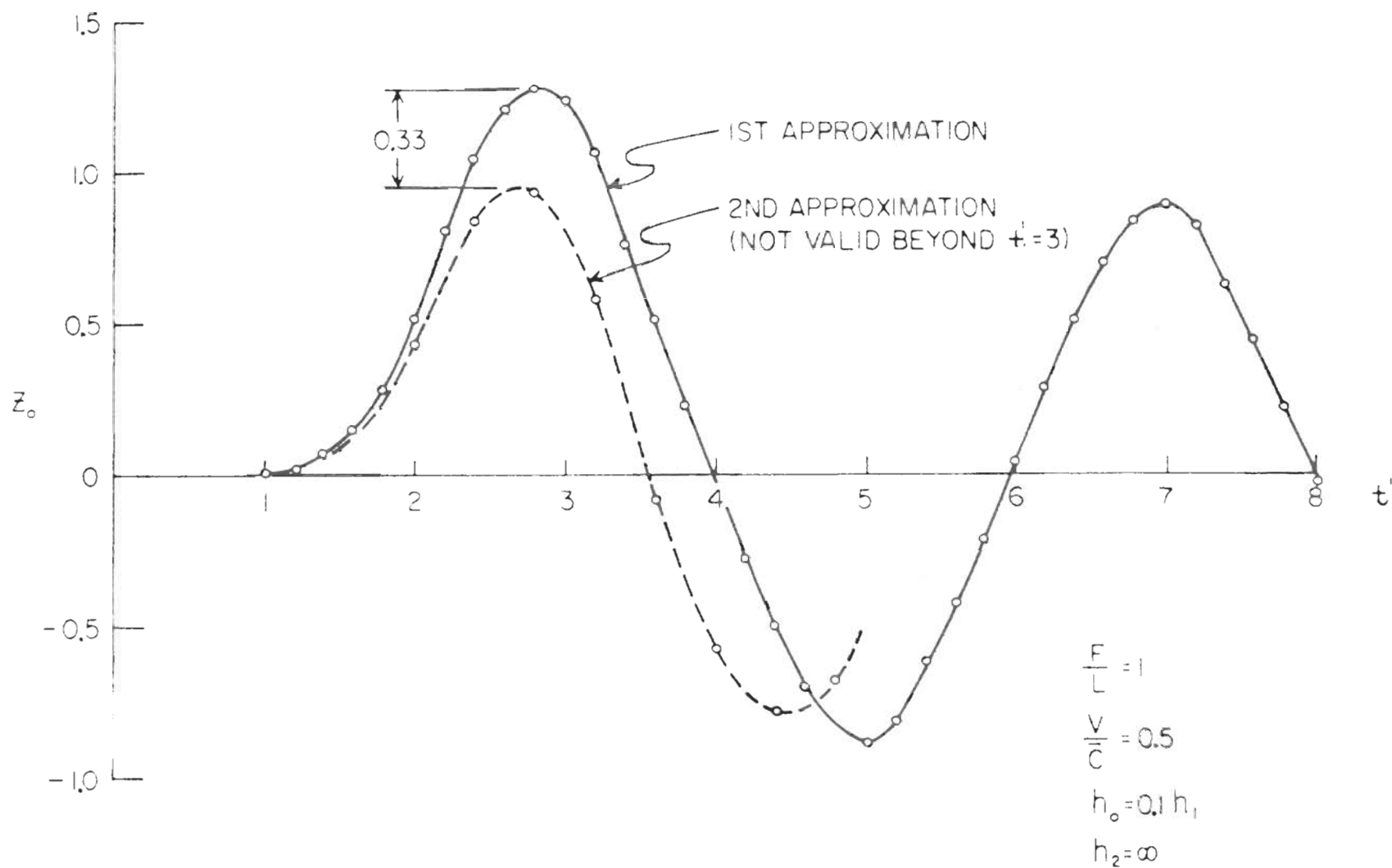


FIGURE 10 · PLOT OF FIRST AND SECOND APPROXIMATION OF Z_0 FOR $V/\bar{C} = 0.5$, $F = L$

allow for finite Z at the edge of the shelf, and require continuity of volume transport and water level at this position then we find that Z and Y must be related by

$$(69) \quad Z_1 = \sqrt{\frac{h_1}{h_2}} Y_1$$

at the edge of the shelf. This assumes that the surge beyond the edge of the shelf is a one-dimensional free surge*. The condition of $Z_1 = 0$ used in all of the previous calculations is a special case of (69) for $h_2 = \infty$. If we take 1200 fathoms as an appropriate value for h_2 off the New England shelf then the boundary condition becomes

$$(69a) \quad Z_1 = 0.224 Y_1$$

(where $h_1 = 60$ fathoms = 360 feet as used previously).

The effect of this modified edge-condition is shown in Figure 11 for the case of $F = L$, $V = 0.5 \bar{C}$. In the upper graph, the values of Z at shore Z_0 and at the shelf's edge (Z_1) are shown versus time t' (dashed curves). The full curve corresponds to the condition of $Z_1 = 0$. Notice that the maximum value of Z_0 is modified only slightly (about 10 per cent), however the free seiche which occurs after the passage of the storm (at time $t' = 4$) diminishes in amplitude considerably with each cycle for the modified edge condition. The physical reason for this is that a significant amount of the reflected energy from shore is being lost across the edge of the shelf.

The lower graph in Fig. 11 shows the variations in Y with time at the edge of the shelf for the two different boundary conditions. The same feature is noticed in these curves, that the difference between them is small during the time that the wind fetch is over the shelf.

Thus it appears from this analysis that the simple boundary condition ($Z_1 = 0$) is evidently adequate for establishing a satisfactory first approximation of the maximum water level, but gives a poor description of the resurgences which follow. The effect of friction and of oblique reflections of the surge at shore (which can only be dealt with in a two-dimensional problem) undoubtedly have a similar effect, in that energy losses from the system occur. Thus energy can be lost by transmission to the deep water, by dissipation (particularly at shore) and by transverse propagation out of the region of shelf concerned. Such modifications should be taken into consideration in a more quantitative study of the water level.

* For a free surge in water of constant depth h_2 , $Q = \sqrt{gh_2\eta}$; this is applied at the position x_1 , thus giving eq. (69).

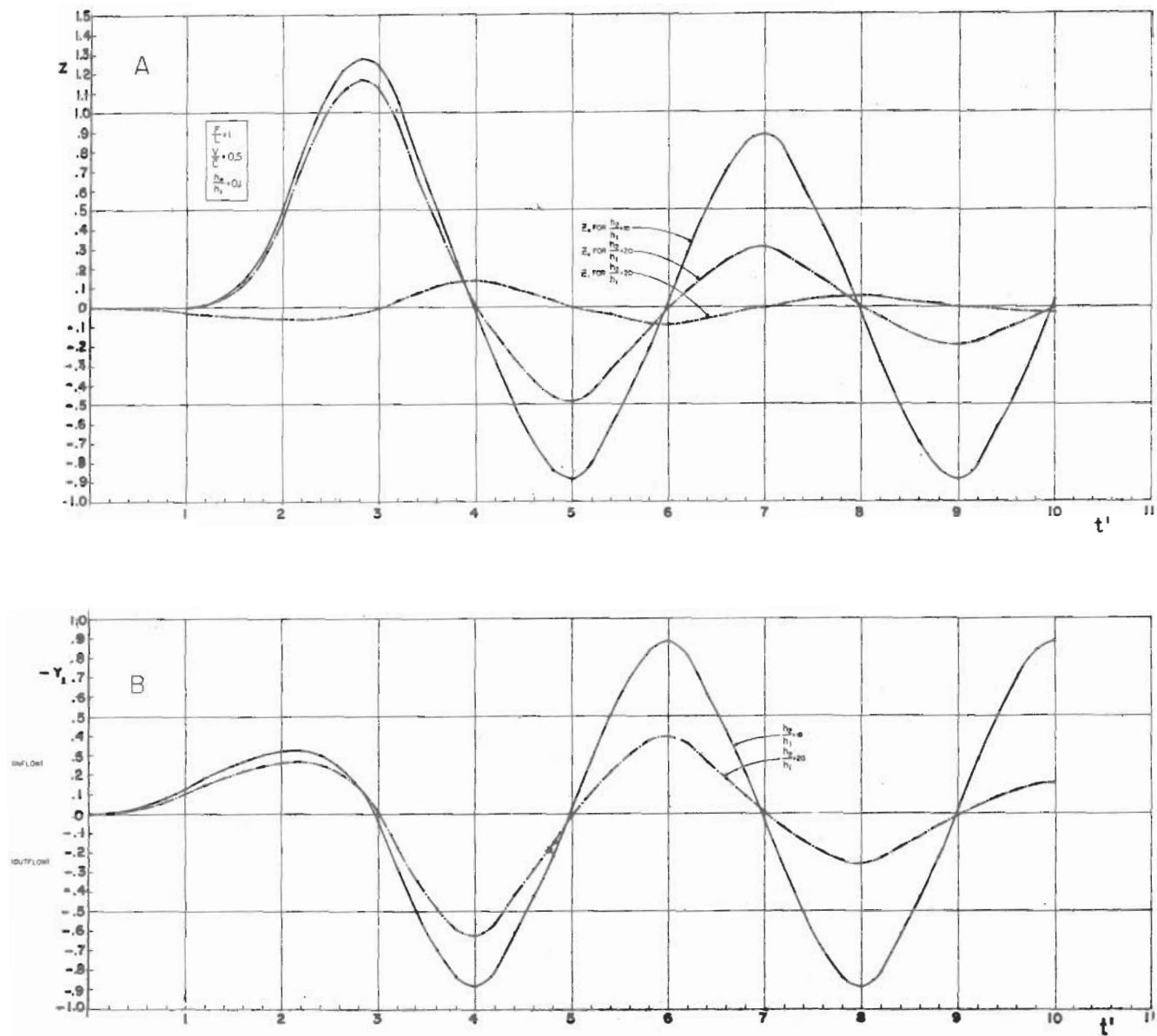


FIGURE 11. COMPARISON OF WATER LEVELS AND VOLUME TRANSPORTS FOR MODIFIED EDGE CONDITION WITH THOSE OF FIRST APPROXIMATION

V. THE RESPONSE DIAGRAM

1. First Approximation Response Diagram.

The values of maximum Z at shore, as determined from the first approximation analysis for different combinations of F/L and V/\bar{C} are summarized in Tables 1-A, B under the heading Z_m . The time of occurrence of the maximum water level at shore is denoted by t_m . This is the elapsed time divided by T reckoned from the time that the front of the fetch crosses the edge of the shelf. Graphs of t_m versus V/\bar{C} for different F/L are given in Figure 14, (page 38).

The time of occurrence of the maximum wind at shore is denoted by t_w ; this is given by

$$(70a,b) \quad t_w = \begin{cases} \frac{\bar{C}}{V} \left(1 + \frac{F}{2L} \right) & \text{for finite fetch} \\ \frac{F}{2VT} & \text{for uniform wind} \\ & (F \text{ and } V \text{ very large}) \end{cases}$$

The differences $t_m - t_w$ are listed in Tables 1-A, B. These represent the relative time of the maximum water stage at shore reckoned from the time of peak wind.

The quantity Δt in Tables 1-A, B represents the "half-life" of the initial surge at shore and is the time interval (divided by T) during which the water stage at shore is greater than (or equal to) half of the maximum value. Graphs of Δt are given in Figure 22, and a schematic indicating how Δt is measured is shown in the upper right portion of this figure. Values of Δt were determined only for those cases for which a complete time plot of Z was constructed. Some of the values are only approximate and are indicated by numbers in parentheses in Tables 1-A, B.

Graphs of the Z_m values versus VT/F for the five different finite fetch lengths are presented in Figure 12. The limiting case of uniform wind (effectively infinite F) is also included for comparison. The abscissa was purposely selected as VT/F so that the limiting case could be included. For most of the cases, the region of the graphs for small VT/F is not defined quantitatively. The oscillatory character of Z_m for small VT/F is well established in the limiting case of infinite F and is indicated in the computations for $F/L = 0.5$. For the other curves, an upper envelope curve has been estimated which terminates at the appropriate steady state value (first approximation value), and the inferred behaviour of the curves are indicated by the dotted lines.

2. Modified Response Diagram.

Figure 12 in effect constitutes a first approximation response diagram. As an improvement over this diagram the values of Z_m were multiplied by a correction factor r which depends upon fetch length. This factor is defined as the ratio of the exact steady state solution to the first approximation steady solution. The values for different fetch length are given in Table 2, below.

TABLE 1-A

SUMMARY OF CALCULATIONS FOR FIRST APPROXIMATION VALUES OF Z_m , TIME OF MAXIMUM, AND HALF LIFE OF SURGE

	F/L = 0.5			F/L = 1.0			F/L = 2.0			F/L = 4.0			F/L = 8.0		
V/\bar{C}	Z_m	$t_m' - t_w'$	$\Delta t'$	Z_m	$t_m' - t_w'$	$\Delta t'$	Z_m	$t_m' - t_w'$	$\Delta t'$	Z_m	$t_m' - t_w'$	$\Delta t'$	Z_m	$t_m' - t_w'$	$\Delta t'$
0	.470	- ∞	∞	.702	- ∞	∞	.961	- ∞	∞	1.122	- ∞	∞	1.22	- ∞	∞
.125	.55	-1.4	3.40												
.16	.61	- .62	3.06	.73	-1.87	5.0	1.02	- .52	7.00						
.20	.45	- .26	4.13												
.25	.50	- .40	2.79	.92	-1.20	-	1.08	-1.5	4.85						
.278	.62	- .6	(2.35)												
.40	.85	- .12	(1.43)	1.23	- .55	-	1.38	- .8	2.46	1.27	- .50	4.70			
.50	.93	- .10	.96	1.28	- .20	1.42	1.57	- .2	1.92	1.26	- .40	-			
.667	1.10	- .08	(.60)	1.34	.05	-	1.66	0	-	1.54	.10	-			
.80	1.18	(- .04)	.41	1.36	.07	(.65)	1.60	0	-	1.69	- .05	-			
1.00	1.20	0	.29	1.33	.10	.60	1.50	.1	1.34	1.84	.10	1.78	1.30	0	4.05
1.33	.85	.16	-	1.12	.18	-	1.34	.2	-	1.66	.15	-	1.57	.05	2.48
1.60	.58	.30	.39												
1.72													1.69	.70	(2.14)
2.00	.36	.43	.52	.64	.30	.57	1.02	.3	.78	1.38	.35	-	1.77	.40	1.85
2.50													1.67	.80	(1.43)
4.00				.23	.12	.83	.48	.3	.87	.80	.35	.93	1.25	.65	-

TABLE 1-B

SUMMARY OF CALCULATIONS FOR FIRST APPROXIMATION VALUES OF Z_m ,
TIME OF MAXIMUM, AND HALF LIFE OF SURGE
UNIFORM WIND FIELD

($F = \infty$)

VT/F	Z_m	$t_m' - t_w'$	$\Delta t'$
.0	1.280	.00	∞
.0450	1.345	.40	
.0469	1.358	.53	
.0490	1.353	.68	
.0511	1.337	.81	
.0536	1.305	.96	
.0563	1.254	.99	
.0592	1.227	.80	
.0625	1.280	.00	
.0662	1.337	.19	
.0704	1.381	.37	
.0750	1.403	.54	
.0804	1.403	.71	
.0866	1.376	.86	
.0938	1.321	.98	
.1023	1.229	.99	
.1125	1.177	.79	
.125	1.280	.00	
.141	1.402	.17	
.161	1.512	.37	
.188	1.588	.54	
.225	1.616	.70	
.250	1.612	.78	1.90
.300	1.573	.89	
.322	1.530	.92	
.347	1.503	.94	
.375	1.444	.97	
.409	1.373	.98	
.450	1.276	.99	
.500	1.150	.80	
1.000	.650	.39	1.88
2.000	.370	.28	
∞	.00	.00	2.00

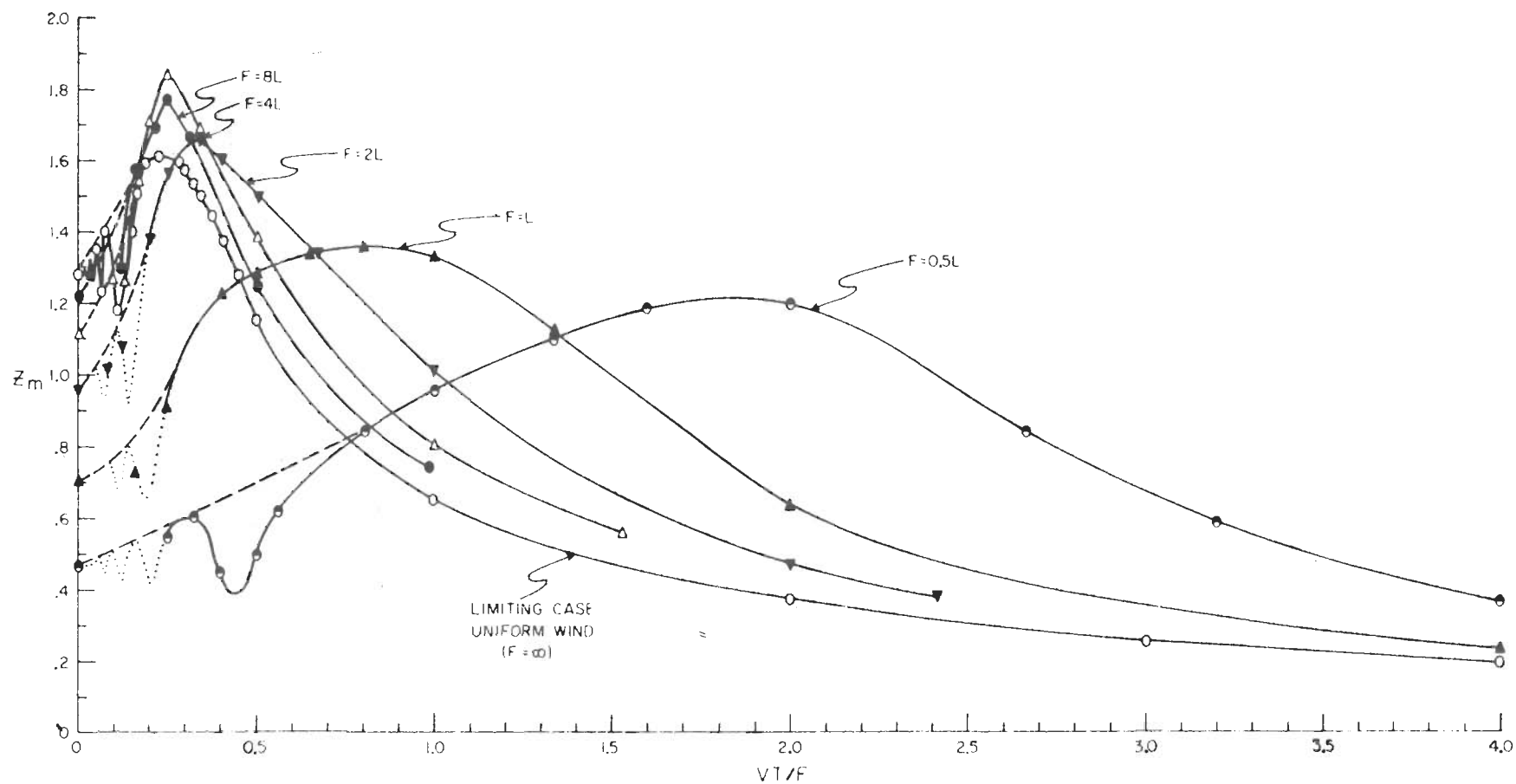


FIGURE 12 • COMPOSITE PLOT OF FIRST APPROXIMATION VALUES OF Z_m VERSUS VT/F FOR DIFFERENT F/L

TABLE 2

CORRECTION FACTOR TO BE MULTIPLIED BY Z_m VALUES

F/L	0	0.2	0.5	1.0	2.0	4.0	8.0	∞
r	1.00	0.905	0.817	0.795	0.755	0.751	0.746	0.739

The modified Z_m values are denoted by the symbol S, i.e.,

$$(71) \quad S = r Z_m$$

These values are considered as better approximations to the true Z_m values and in fact are the exact Z_m in the steady state case. For the case of $F/L = 1.0$, $V/\bar{C} = 0.5$ which was investigated in some detail, the value of S is 1.02 which is just slightly above the second approximation value for Z_m (see Figure 10). This certainly substantiates the use of the correction factor r for this case.

The final response diagram is given in Fig. 13. This shows isolines of S on a graph of F/L versus V/\bar{C} where it will be recalled that F is the actual fetch length, L is the width of the shelf, V is the actual velocity of the storm (assumed constant) and \bar{C} is the mean free-wave speed:

$$(72) \quad \bar{C} = \frac{1}{2} (\sqrt{gh_0} + \sqrt{gh_1})$$

The scales for F/L and V/\bar{C} are logarithmic so that the limiting case of uniform wind field (very large F) appear as straight isolines of S with unit slope. The maximum value of S for the limiting case is slightly less than 1.20. The important feature of this diagram is that the ultimate maximum of S (hence of water level at shore) occurs at a finite fetch length, the value of maximum S being just about 1.40.

The region where the secondary resonances in response occur is shown by dashed lines, since the computations were insufficient in number to determine this phenomenon quantitatively, except for two limiting cases. These secondary resonances are all less than that of the primary resonance at $F/L = 4$, $V/\bar{C} = 1$ and diminish in amplitude in the approach to steady state. Steady state limits for S are indicated on the left hand margin of the graph and apply strictly to the case where $V = 0$.

3. Use of the Response Diagram.

From a knowledge of the fetch length F, the storm speed V, and the shelf dimensions we can determine the appropriate value of S from Fig. 13. The approximate maximum water level at shore is accordingly given by

$$(73) \quad \eta_m = \frac{U^2 T}{C_1} \left(\frac{h_1}{h_0} \right)^{1/4} S$$

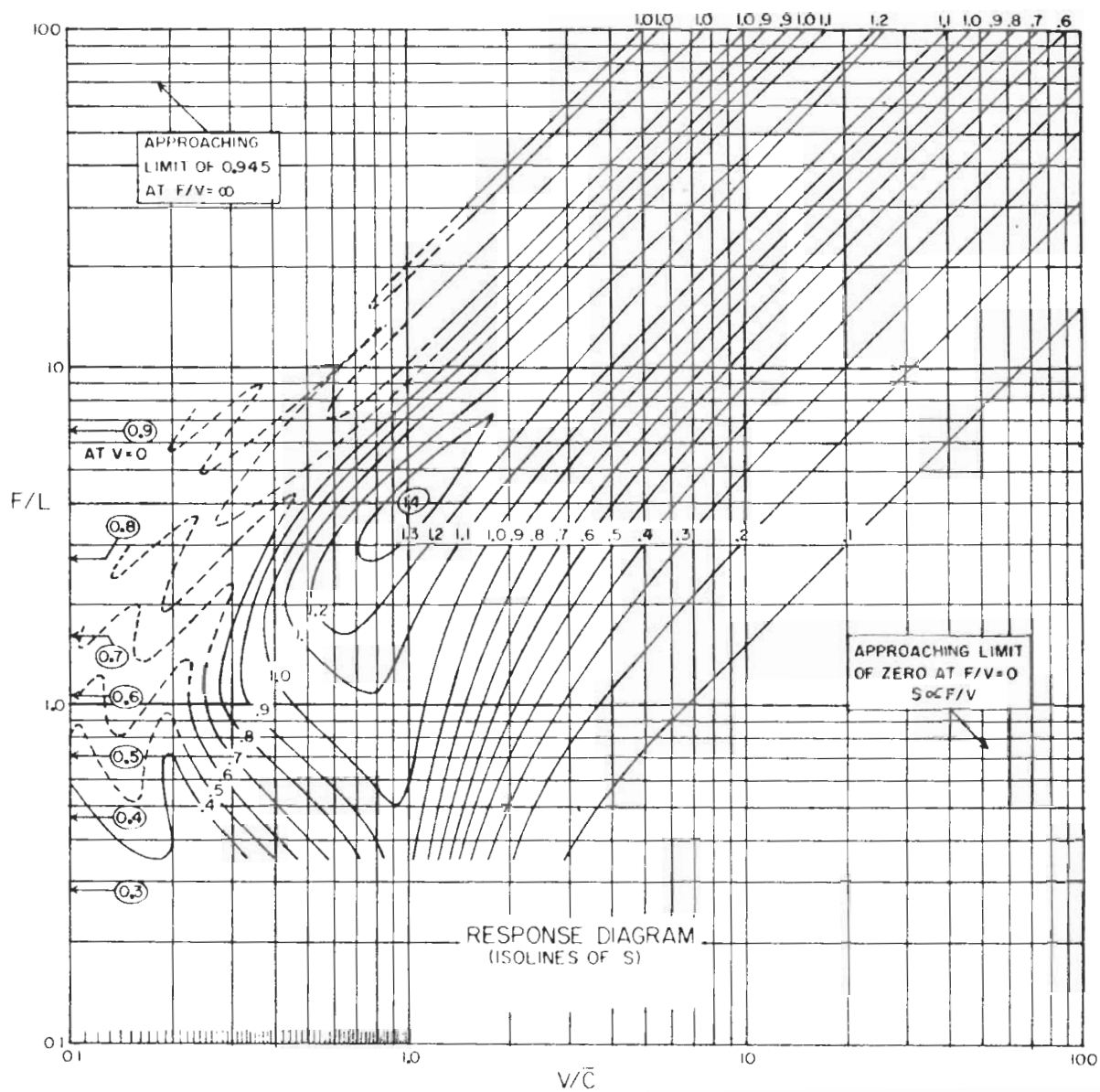


FIGURE 13 · RESPONSE DIAGRAM: ISOLINES OF S VERSUS F/L AND v/\bar{c}

It will be recalled that ρU^2 is the maximum value of shoreward wind stress in the fetch. We can take this in the form

$$(74) \quad U^2 = K W_m^2$$

where K is a dimensionless coefficient and W_m is the maximum wind speed (if the latter is directed towards shore). The coefficient K is related to the usual resistance coefficient * k by the relation

$$(75) \quad K = \frac{\rho^* k}{\rho}$$

where ρ^* is the density of air at sea level and ρ is the density of sea water. The results of laboratory tests of wind stress and of the experiments at Lake Okeechobee indicate that K is of the order of 3×10^{-6} . The exact magnitude of this coefficient is not of immediate concern here, but will be in later calculations concerning the design storm. The important assumption is that K is considered constant at least for wind speeds of storm intensity.

Taking U^2 in the above form gives

$$(76) \quad \eta_m = \left[K \frac{T}{C_1} \left(\frac{h_1}{h_0} \right)^{1/4} \right] W_m^2 S$$

If we select $h_0 = 36$ feet, $h_1 = 360$ feet, $L = 84$ nautical miles, we obtain

$$\begin{aligned} C_0 &= 23.1 \text{ mph} \\ \frac{C_1}{C_0} &= 73.1 \text{ mph} \\ \frac{C_1}{C} &= 48.1 \text{ mph} \\ T &= 2.01 \text{ hours} \end{aligned}$$

Taking $K = 3 \times 10^{-6}$ gives

$$(77) \quad \boxed{\eta_m \doteq 7.7 \times 10^{-4} W_m^2 S}$$

where η_m is in feet and W_m is in mph.

* Usually stress is expressed in the form $\tau = \rho^* k W^2$.

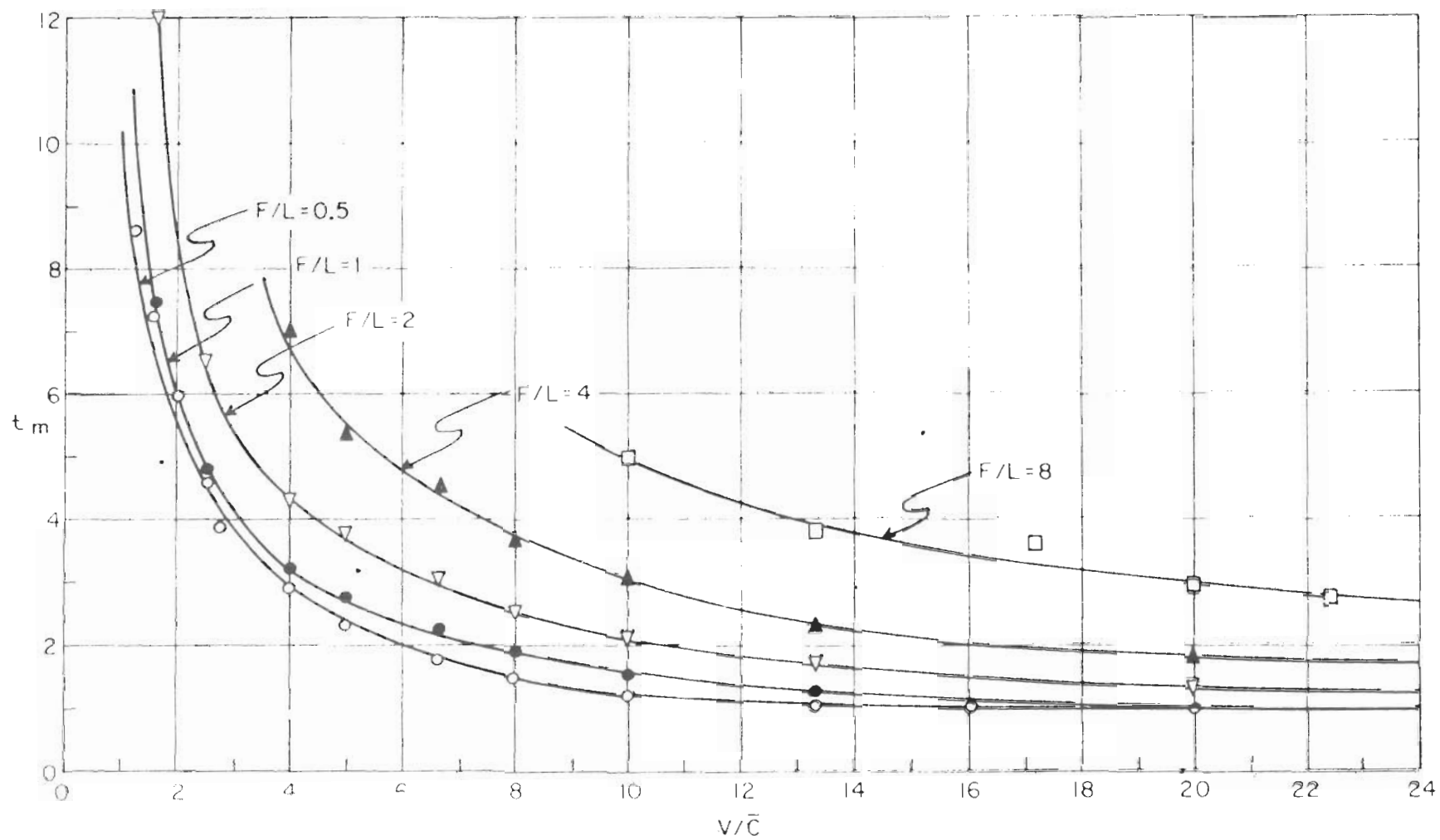


FIGURE 14 • RELATIVE TIME OF MAXIMUM WATER LEVEL AT SHORE

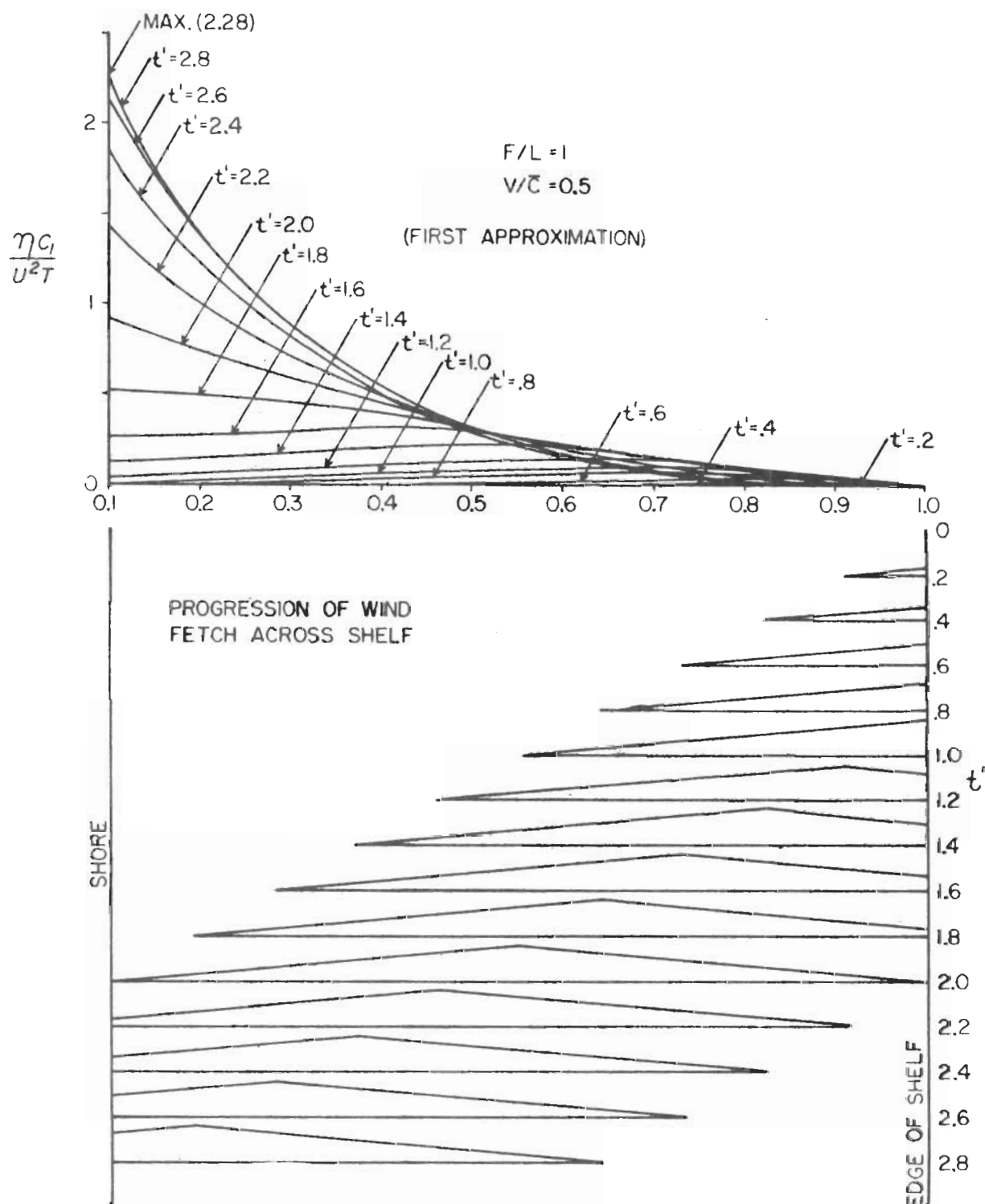


FIGURE 15 • GENERATION STAGE OF SURGE FOR THE CASE
 $V/\bar{C} = 0.5$, $F = L$

VI. EVALUATION OF STORM TIDE POTENTIAL FOR PAST STORMS

1. Evaluation of F and W_m .

In order to apply the present theory to an actual storm it is necessary to determine the components of wind stress along a line normal to the coast. Since it is assumed that the wind stress is proportional to W^2 (and in the same direction as W) it follows that the component of wind stress in the x direction is given by

$$(78) \quad \tau = \rho K W^2 \cos \theta$$

where θ is the angle between the wind vector and the x axis. Now since $W \cos \theta$ is the component velocity of wind in the x direction (W_x) we can write

$$(79) \quad \tau = \rho K W W_x$$

Three hurricanes have been analysed in detail. The dates of these are September 21, 1938, September 14, 1944, and August 30, 1954 (Carol). The distributions of wind speeds and directions for these storms were ascertained from data supplied by the Hydrometeorological Section of the Weather Bureau in memoranda from Mr. C. S. Gilman to the Chief of Engineers dated November 18, December 1, and December 2, 1955. A graph of the mean variation of the angle ψ (Fig. 16) with radial distance r (established from the 1938 storm data, by the Hydrometeorological Section) was used together with the angle θ to determine appropriate values of θ for calculating W_x .

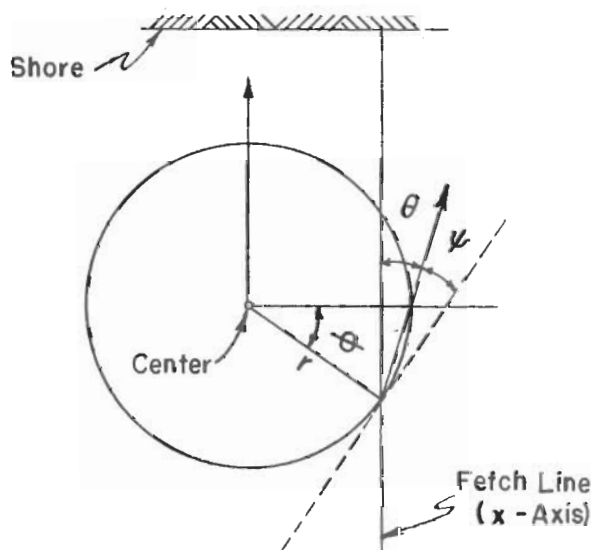


FIGURE 16 · SCHEMATIC OF STORM SHOWING ANGLES θ , ϕ AND ψ

For all three storms the fetch line was selected parallel to the direction of motion and taken through the region of peak wind speed (see Figure 20 as an example). Only in the case of the 1938 storm was the path nearly normal to the coast, and in this case the chosen fetch line does not line up directly with Narragansett Bay. However in order to determine the most severe conditions for the particular storm in question it is assumed that this fetch could have occurred normal to the coast off Narragansett Bay. Thus the resulting calculations lead to a storm tide potential rather than an estimate of the tide for the particular path followed.

2. The Storm Tide Potentials.

The calculated values of WW_x for the three storms are shown in Figs. 17, 18 and 19 (full lines). The fitted model is shown by the dashed lines. The departure from the model distribution at the rear of the storm is not serious since the maximum water level occurs prior to the passage of this section of the fetch at shore. The value of W_m pertaining to each fitted curve was taken as $\sqrt{(WW_x)_{\max}}$. The value of V for each storm was taken as the mean propagational speed along the path for one day in the vicinity of 41° North latitude. These were evaluated by the Hydrometeorological Section of the Weather Bureau. Values of F , W_m , and V are summarized in Table 3. The quantities F/L and V/\bar{C} were computed using $L = 84$ nautical miles and $\bar{C} = 48$ mph and the appropriate values of S were obtained from Figure 13. The estimated storm tide potential as computed from equation (77) is listed under η_m .

TABLE 3

COMPUTED STORM TIDE POTENTIALS

Hurricane	F (n. mi.)	W_m (mph)	V (mph)	F/L	V/\bar{C}	S	η_m (ft)
Sep. 1938	148	88	42	1.76	.88	1.16	6.9
Sep. 1944	124	84	33	1.48	.69	1.17	6.4
Aug. 1954	87	95	32	1.04	.67	1.08	7.5

The maximum tide observed in Newport Harbor for the 1938 hurricane was about 7.5 feet above predicted*. The effective head due to barometric pressure lowering is about one foot which when subtracted from the above value gives about 6.5 feet for the effect of wind and inertia of the water.

For comparison with the above figures (Table 3), the most severe conditions according to Figure 13 are for $F = 340$ nautical miles and $V = 48$ mph (42 knots) in which case $S = 1.40$. For $W_m = 100$ mph this gives

* Supplemental Report on Hurricane of September 21, 1938, Corps of Engineers, U.S. Army, Providence, R.I., June 1939 (Figure of tide curve for Newport).

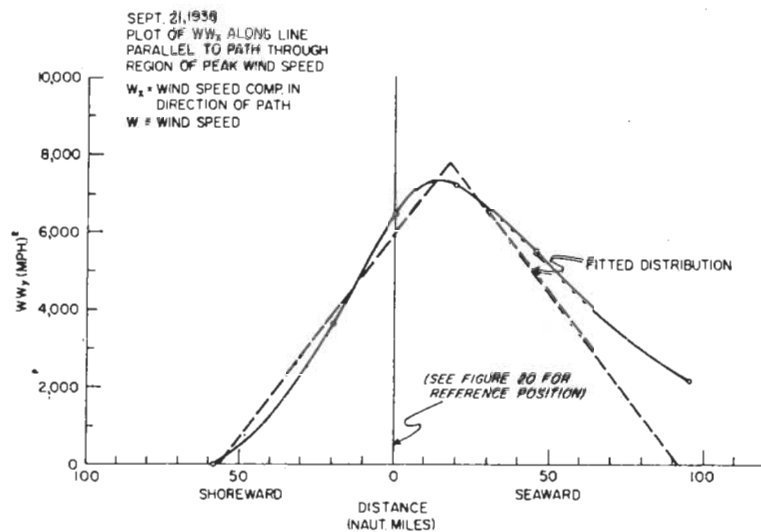


FIGURE 17 - PLOT OF WW_x ALONG LINE PARALLEL TO PATH
THROUGH REGION OF PEAK WIND SPEED FOR
HURRICANE OF SEPTEMBER 21, 1938

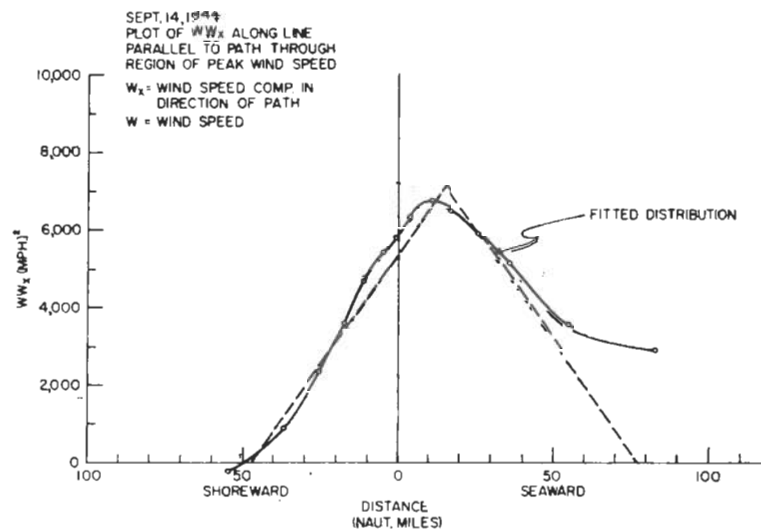


FIGURE 18 - PLOT OF WW_x ALONG LINE PARALLEL TO PATH
THROUGH REGION OF PEAK WIND SPEED FOR
HURRICANE OF SEPTEMBER 14, 1944

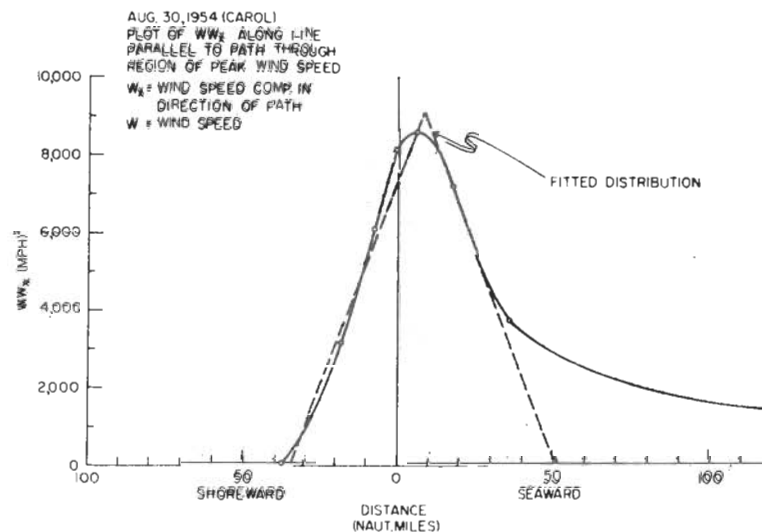


FIGURE 19 - PLOT OF WW_x ALONG LINE PARALLEL TO PATH
THROUGH REGION OF PEAK WIND SPEED FOR
HURRICANE OF AUGUST 30, 1954

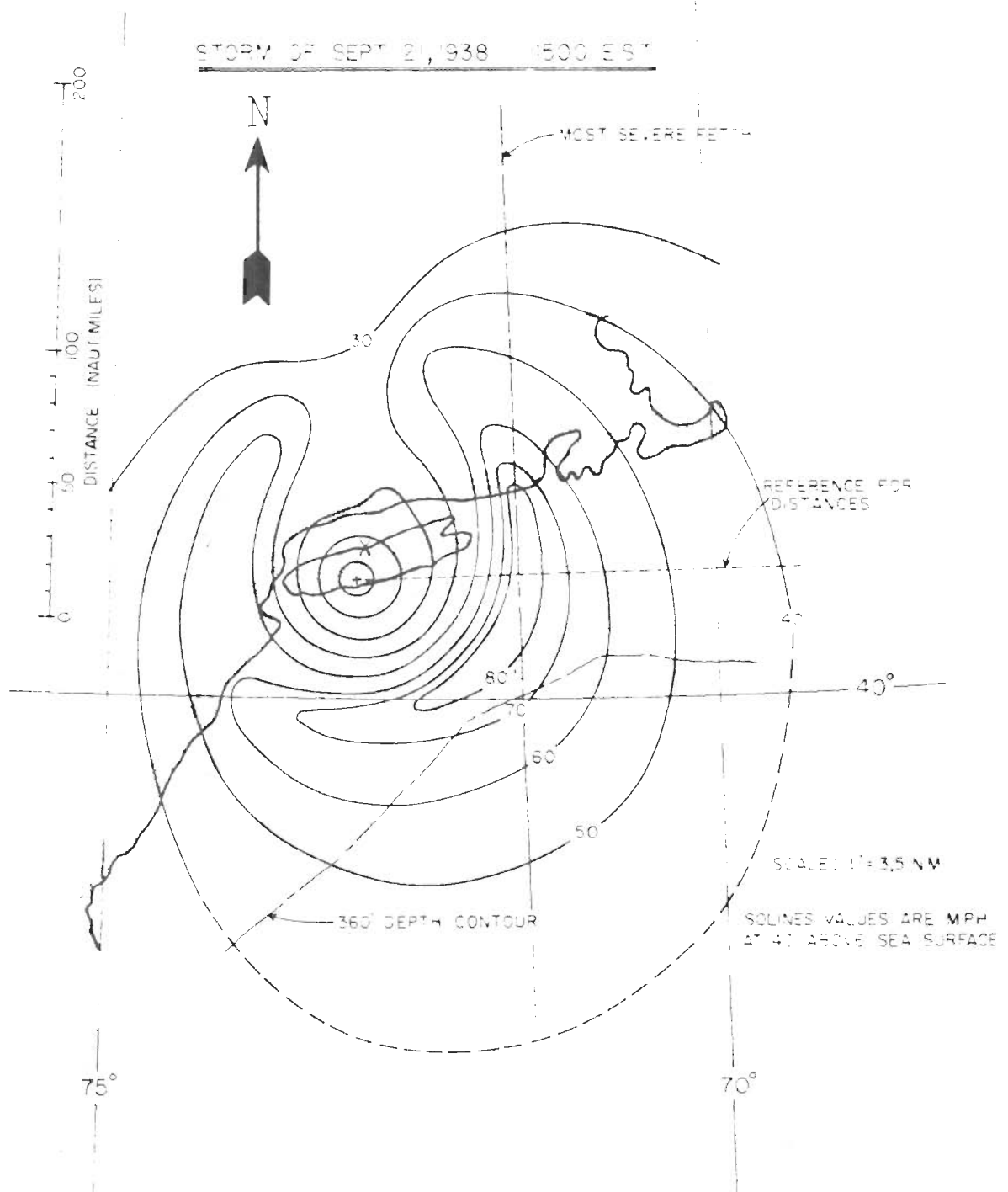


FIGURE 20 • SURFACE WIND ISOLINES FOR HURRICANE OF SEPTEMBER 21, 1938 - 1500 E.S.T.

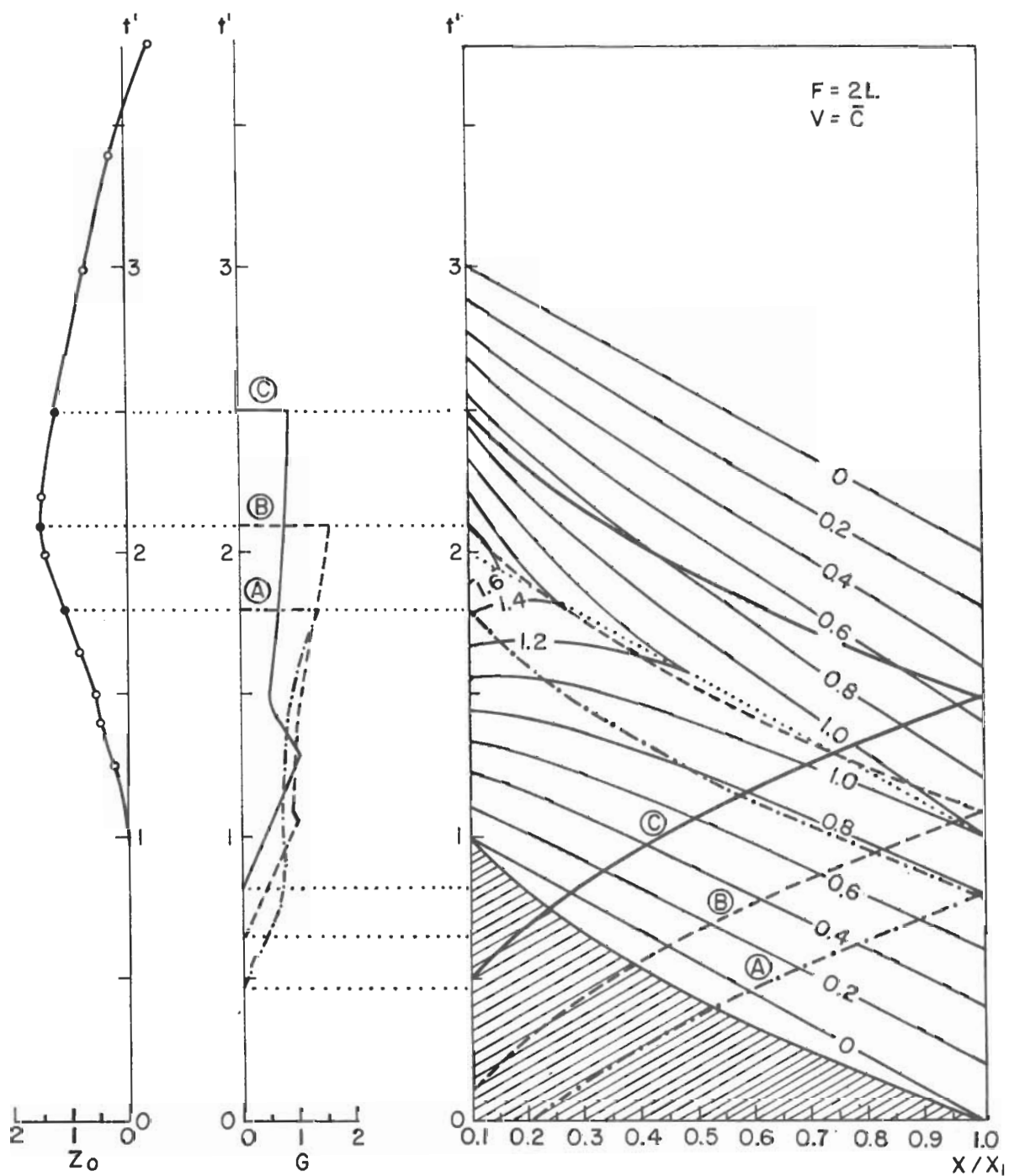
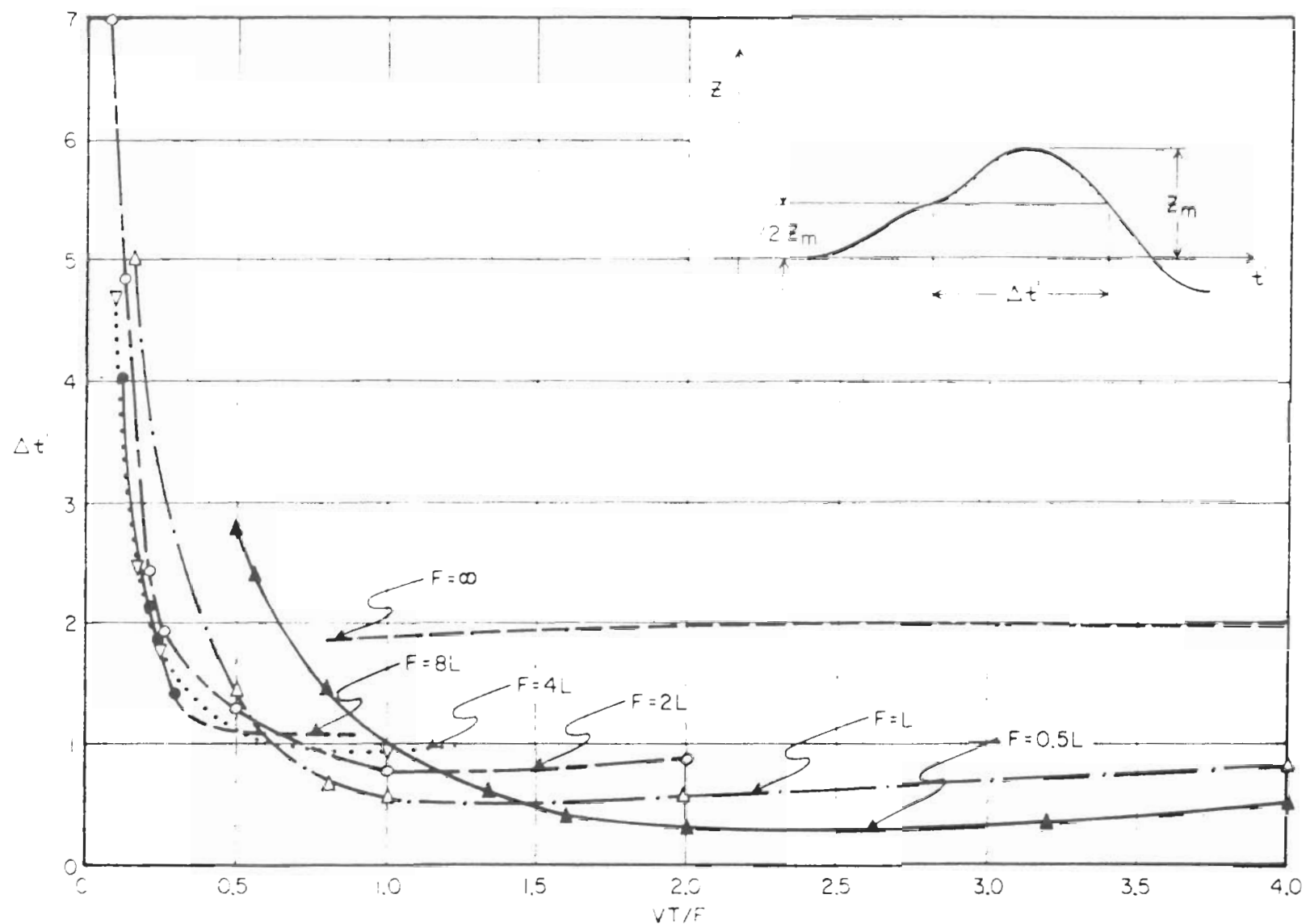


FIGURE 21 · EXAMPLE OF COMPUTATION OF Z FOR $F = 2L$, $V = \bar{C}$

FIGURE 22 · HALF LIFE VERSUS VT/F FOR DIFFERENT FETCHES

a value of η_m equal to 10.8 feet above and beyond ordinary tide and low pressure effects. It must be borne in mind that all of the values of η_m given here apply to the open coast or bay mouth. Within the bays additional amplification will result from convergence and direct piling up by winds over the shallow water of the bay.

3. Comparison of R and F.

Observed values of the distance (R) from storm center to region of maximum wind for the three hurricanes examined above were supplied by the Hydrometeorological Section. These give the following values for the ratio F/R: 2.47, 3.05 and 3.95 for the 1938, 1944, and 1954 hurricanes respectively. This set is really insufficient for determining a reliable value of the ratio. However if we take a mean of 3.4 then the R value which yields the greatest storm tide potential for a storm of given peak wind speed is 100 nautical miles.

4. Suggested Method for Selection of Most Severe Storm.

It was shown in Hydrometeorological Report No. 32 (1954, p. 27) that the maximum wind speed at gradient wind level in a hurricane is nearly proportional to $\sqrt{\Delta p}$ where Δp is the depression of central pressure below normal. If we consider that η_m is likewise proportional to $\sqrt{\Delta p}$ then from equation (77),

$$(80) \quad \eta_m \propto (\Delta p)^S$$

For any given relative fetch length (F/L), there exists an optimum value of V/C for maximum S. The function $S_m(F/L)$, where S_m is such a maximum, can be ascertained from Figure 13. For example if F/L = 1.0 then S is a maximum at V/C = 0.8 and has the value 1.08; while if F/L = 2.0 then S is a maximum at V/C = 0.65 and has the value 1.23, and etc.

If we consider that F is proportional to R and suppose that an upper limit of R can be defined for a storm of given Δp from a scatter diagram of R versus Δp for different hurricanes, then S_m can be established as a function of Δp , for a given shelf width L. Now if we evaluate the product $\Delta p S_m$ for different values of Δp we can determine the optimum value of Δp which gives a maximum value of the above product and hence of η_m . This optimum Δp together with the associated R or F value could then be used as gross parameters by which to characterize the most severe hurricanes in respect to coastal water level according to the present theory.

ACKNOWLEDGEMENT

The author wishes to express his appreciation of the assistance of R. G. Dean, K. Kajiura and H. E. Schildknecht in carrying out the graphical and numerical work. Special credit is due to K. Kajiura for his valuable assistance and suggestions in regard to the theoretical work.

REFERENCES

1. Freeman, J. C., The Solution of Non-Linear Meteorological Problems by the Method of Characteristics, Compendium of Am. Met. Soc., 1951, pp. 421-33.
2. Gilman, C. S., Memos to Chief of Engineers from the Hydrometeorological Section, U. S. Weather Bureau, Nov. 18, Dec. 1, Dec. 2, 1955.
3. Lamb, Horace, Hydrodynamics, Dover, 1945.
4. Reid, R. O. and B. W. Wilson, Compendium of Results of Storm Tide and Wave Analysis for Full Hurricane Conditions at Freeport, Texas, Final Report to the Dow Chemical Company, Ref. 54-6F, A. & M. College of Texas, Dec. 1954.
5. Supplemental Report on Hurricane of September 21, 1938, Corps of Engineers, U. S. Army, Providence, R. I., June 1939, (Figure 20).
6. U. S. Weather Bureau, Characteristics of U. S. Hurricanes Pertinent to Levee Designed for Lake Okeechobee, Florida, Hydrometeorological Rep. No. 32, Washington, D. C., March 1954.

9622, 032